Response to reviewers

General Comments

We are very grateful for each reviewer's input and have adjusted the manuscript accordingly. Outlined below are the major changes we have made, followed by specific responses to each reviewer. Thank you to everyone involved.

Major Changes:

- Further emphasize the aquaplanet's ability to generate realistic blocks, comparing them to results from reanalysis and idealized model integrations with orography (Section 3.1 of the revised manuscript)
- Removal of the midlatitude vs. high latitude blocking subsection
- Switched the orographic configurations that are analyzed to instead be single mountain configurations of varying height, and just one two-mountain configuration.
- Removal of the analysis on block displacement
- Refocusing of the questions being addressed of this paper (as per the suggestions of reviewer 2):
    1. Are blocks in an aquaplanet dynamically similar to blocks in orographically forced simulations and reanalysis?
    2. Does the presence of orography affect the overall frequency of blocking?
    3. How does orography affect the spatial distribution of blocking frequency?
    4. Does orography affect the duration of blocking events?

Reviewer feedback led us to a better appreciation of the aquaplanet results (i.e. Reviewer 2 – General Comment 3, Reviewer 3 – Major Comments 1 and 3). Therefore, we have further emphasized this section and included results that compare how blocking in an aquaplanet relates to blocking in the real-world and idealized model configurations with topography (Fig. 3).

With regards to the midlatitude vs high-latitude blocking results from the original submission, we received mixed feedback from the reviewers (i.e. Reviewer 2 -- General Comment 2, Reviewer 3 Major Comment -- 2). We acknowledge the dissimilarities between blocks in the midlatitude and high-latitude blocks, especially with regards to wave activity flux, however, we do not want to distract from the primary focuses of this paper. We have opted to remove this analysis.

Motivated by Reviewer 2 – General Comment 1, to mitigate difficulties from the interference of forcing from multiple mountains, we now choose to analyze a different set of idealized model configurations with topography. For this, the results from single mountain configurations of varying height are presented as the new primary focus. Results from the original two-mountain configuration with zonally asymmetric spacing between the mountains are also briefly presented to reaffirm results from the single mountain analysis. Overall, the main points remain the same. Topography leads to:

1. An overall hemispheric increase in blocking frequency
2. The anchoring of regions of enhanced and suppressed blocking frequency
3. The suggestion of regions of enhanced blocking duration

To minimize redundancy, the results from the configuration with zonally symmetric spacing between the mountains from the original submission is now omitted. The discussion of the spacing of mountains having an effect on the spatial distribution of block frequency has also been removed and will be explored in future work.

The analysis on block displacement was motivated by the changing length of the ocean basins used in the previous iteration of this paper. This ended up being a very short section that produced a null result. The switch in topographic configurations now used in the revised article offers little relevance to the displacement analysis. Furthermore, we do not want to distract the reader from the overall main points of this article. The block displacement analysis is now removed.

Response to Reviewer 1

General comment:

This paper studies the topographic effect on blocking formation, using an idealized GCM. The authors have done aquaplanet simulations and simulations with different types of topographies (idealized mountains). They compared the simulation results with and without topographic forcing to demonstrate the influences of topography on blocking formation in terms of dynamics, spatial frequency, duration and displacement. They conclude that the simulation results have important implication for understanding blocking dynamics in the real atmosphere. Overall, the paper is interesting and clearly written, and it would certainly improve our understanding in blocking dynamics, which suddenly became a hot research topic in recent few year. I would recommend publication with minor revision. My comments in the following are for the authors' reference.

[Ans] Thank you for your feedback, we hope to have addressed your criticisms below to satisfaction. Note, any comments regarding typographical errors are skipped over here, but integrated into the manuscript.

Specific comments:

1. *In the simulation by Hu et al. (2008), solar insolation is fixed at March equinoctial condition. It generates greater meridional temperature gradients in the middle and upper troposphere and thus stronger baroclinic eddies. This could be the reason why there are frequent blocking events in their simulations. In the present study, if insolation has seasonal variations, it would be good to look at whether there are seasonal variations of blocking frequencies.*

   [Ans] Compared to previous studies (Tibaldi et al. 1994, MWR; Barriopedro et al. 2010, Clim. Dynam.), we observed a similar seasonal cycle in blocking within our idealized model integrations (i.e. block frequency peaking within NH DJF or SH JJA, see figure below) but some configurations had shifts of about 1 month. To avoid ambiguity, we have chosen to change our seasonal sorting from "winter" defined as DJF, to "cool season" defined as NDJFM.

   With regards to Hu et al., they find more blocking events compared to Weidenmann et al. (2002, JoC) which uses reanalysis. This is tricky to interpret however, as Weidenmann et al. (2002, JoC) counts blocks from all seasons, including summer, which has been shown to have considerably less blocking than winter (Tibaldi et al. 1994, MWR; Barriopedro et al. 2010, Clim. Dynam.). Furthermore, Hu et al. utilizes a different block tracking algorithm from Weidenmann et al., where it has been shown that different tracking algorithms each have their own biases with respect to block frequency (Barnes et al. 2011, Clim. Dynam.). We now elaborate a bit more on this in the introduction (see lines 49-55 of the revised manuscript).

   Hu et al. speculates this increase in frequency in their model is from stronger forcing from transient eddies. We have yet to explore that in the aquaplanet used here, but the enhanced blocking frequency in the idealized model used here is consistent with an overall weaker jet (see Figs. 4b and 5c-d in the revised manuscript), and thus enhancement of blocking (see Nakamura and Huang 2018, Science).

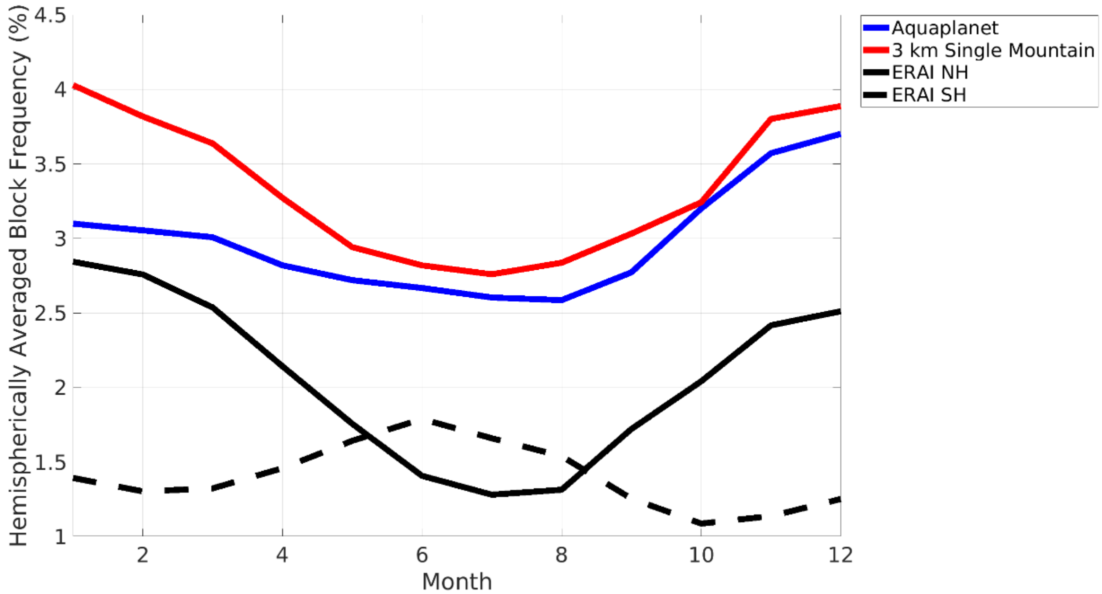

2. *It would be good if the authors add a couple of sentences about why the mountain size of 15 degrees in latitude and longitude is chosen. Is it large enough to generate stationary waves?*

   [Ans] Good point, this mountain size was chosen following Lutsko and Held (2016, JAS). Our results show that it is certainly large enough to generate a considerable stationary wave (Figure 6). We hope this is clearer in lines 103-105:

   "Like Cook and Held (1992), and following Lutsko and Held (2016), perturbations to the surface height are introduced in the form of Gaussian mountains centered at 45° N with half-widths of 15 degrees in both the latitude and longitude dimensions."

   It would be interesting to investigate the atmospheric response to mountain width in the future.

3. *Line 247: Why do you choose the 85% confidence level? Is it too low? People usually use at least the 90% confidence level.*

   [Ans] We received similar feedback in the other reviews. After further self-clarification we have now chosen a 95% confidence interval and more careful wording to describe quantitative differences throughout our analyses. See the methods subsection 2.5.4, lines 256-257:

   "A 95% confidence interval is imposed as the significance threshold for all significance testing."

5. *Line 108: Q-flux, is there horizontal heat flux?*

   [Ans] No, there is no horizontal heat flux in the oceans of the idealized model integrations used for this paper. To avoid ambiguity, we replace this line about horizontal heat fluxes with a clearer description of what no Q-flux actually means in lines 112-114:

   "Ocean grid cells are represented using a slab ocean with a depth of 20 m. For simplicity we prescribe uniformly zero Q-flux, meaning that we assume that in the time mean, the net flux of energy from the ocean to the atmosphere is zero at all surface grid cells."

6. *Section 2.4: there are too many short paragraphs. It would be good to put them together.*

   [Ans] We have slightly restructured this section combining the explanation of the stationary wave and storm track into one subsection (2.4.1), and the blocking and zonal wind climatologies into another (2.4.2). These fields are grouped together in a consistent way in which they are presented in Figure 4-7, and 9.

7. *Line 505: surface forcing –> topographic forcing 8. Lines 537 and 545: "resonance" may not be a good terminology. It is actually nonlinear eddy-eddy interaction or interaction between transient waves and stationary waves.*

   [Ans] Agreed, this is now removed.

8. [Ans] In original review there was no comment 8.

9. *Fig. 4b: I am confused by this plot at beginning, and I thought blockings occur at the equator. It is good to pointed out in the figure caption that the reference latitude is removed.*

   [Ans] We have updated the figure caption for the revised submission (Fig. 3). We hope the line we added at the very end better clarifies things:

   "Figure 3: For cool season blocking events: Block centered composites of positive 500 hPa geopotential height anomalies (solid contours), negative 500 hPa geopotential height anomalies (dotted contours), $\vec{W}$ (arrows), and $\nabla \cdot \vec{W}$ (shading). (a-c) Left: Computed with SH blocks in ERA-Interim. (d-f) Centre: Computed with blocks in the aquaplanet integration. (g-i) Right: Computed with blocks in the 3 km single mountain integration. The top, middle, and bottom rows are composites over the first, strongest, and last timesteps of blocking episodes, respectively. Positive (negative) 500 hPa geopotential height anomaly contours are in 50 m (-10 m) intervals with outer contour 50 m (-30 m). $\vec{W}$ with magnitudes less than 20 m^2 s^{-2} are removed. **Latitude and longitude are defined relative to the composite block center**"

Response to Reviewer 2

Summary:
Scientific significance: Fair
Scientific quality: Fair
Presentation quality: Fair

This paper uses an idealized aquaplanet model to compare statistics of atmospheric blocking between configurations with zonally symmetric and asymmetric surface boundary conditions. Zonally asymmetric boundary conditions change the spatial location, frequency, and duration of blocking in comparison to the zonally symmetric configuration, consistent with changes in climatological storm tracks and stationary waves. The results suggest zonally asymmetric surface boundary conditions control the spatial distribution of blocking in the real atmosphere to first order.

I think this paper is interesting and the results are relevant to this journal. However, I think the Paper:
1) does not provide sufficient explanations for the questions posed
2) needs to focus more on the key results
3) does not consider a key implication of the experiments which was proposed in previous work.

Therefore, it is for these reasons, which are summarized in more detail below, which I recommend major revisions before this paper can be published.

[Ans] We acknowledge and find validity in these criticisms. To address them, as summarized in the cover letter, in broad terms we have:

- Reformulated our questions to address key results
- Provided greater detail in our explanations to connect our results to previous work
- Modified the selection of topographic configurations to vary topography in a way that has less degrees of freedom than the original set
- Updated the selection and presentation of the dynamical fields chosen for the results presented (i.e. presenting wave activity flux divergence instead of magnitude, presentation of climatological U250 with blocking climatology, etc.) Specific details of this are given below

General comments:

1. *I don't think the paper provides sufficient explanations for the questions posed (e.g. lines 344-346 and 483-487). Specifically, the explanations are generally qualitative and show consistency between different fields (e.g. storm tracks, stationary waves and blocking) and the authors often state that future work is required to understand the causal mechanisms (e.g. lines 443-445, 457-458, 492-493, 556-558). While it is clear that the surface boundary conditions cause the changes in blocking, it is difficult to establish the exact mechanisms because everything is changing at once. Therefore, I'm not sure the*

authors can answer the questions posed with these simulations only. It likely requires more detailed analysis with regards to the theories discussed in the introduction or more experiments with simpler models.

[Ans] This comment is addressed by the modification of the research questions and set of topographical configurations that are analyzed. Reviewer comments reflected the importance of the aquaplanet results, hence the reformulated question 1. For this, block centered compositing is utilized for the aquaplanet, topographic configurations, and reanalysis (Fig. 3, section 3.1)

With regards to the notion of using simpler models, we have opted to present an analysis for a different set of topographic configurations. The new configurations are a set of single mountain integrations with varying max surface heights (1 km, 2 km, 3 km, 4 km) and one integration with two identical 3 km mountains. The revised manuscript also contains more explicit reference and connection to previous work (namely Nakamura and Huang 2018 Science, Nakamura et al. 1997, Takaya and Nakamura 2001)

2. *I think the paper would benefit from focusing more on the key results. For example, I'm not sure how the analysis of high-latitude versus low-latitude blocking relates to the experiments because the authors state that the results are similar in all simulations and reanalysis (lines 296-299) and blocking is much less frequent in high-latitudes (Fig. 4a). The authors devote a significant portion of the results to discussing the reanalysis and model climatological stationary waves, storm tracks and jets (lines 306-404) which could be summarized in a few sentences since these features are well known and the responses are well understood. Finally, the subsampling analysis in Fig. 7 could also be discussed in words only and the case study in Fig. 1 could be omitted altogether since similar results are presented in Fig. 2.*

[Ans] The midlatitude vs. high-latitude blocking analysis is now removed. The aquaplanet results are more focused to investigate the dynamical representation of blocking across models (Fig. 3, section 3.1)

The section regarding model climatological responses (lines 306-404 of the original manuscript) has been made to be more concise (section 3.2.2). We still choose to keep this part to affirm our methodology and set the table for the analysis that comes after using the idealized model. We remove Fig. 7 and merge the presentation of aquaplanet convergence with Fig. 4, which is now discussed in section 3.2.1.

Regarding your suggestion of removing figure 2, we choose to keep figure 2 to provide the reader with a quick reference to what the blocks look like on an individual basis, not just in composites. Also, figure 2 provides a snapshot of the characteristic overturning of Z500 contours (a.k.a. wave-breaking) associated with blocking, which supports the idea of this model generating realistic events.

3. *I think the paper does not consider a key implication of their results which was proposed by Hu et al. (2008). Viewed from their perspective, the results presented here demonstrate that zonally symmetric models capture the key features of blocking. To be clear, the results show that the surface boundary condition controls the spatial distribution of blocking. However, I was surprised to see that many of the hemispheric*

statistics listed in Tables 2-4 show modest changes on the order of 10-30% when topography is included. Moreover, the composite analyses in Figs. 3 and 9 suggest the dynamics of individual blocks are similar with and without topography. I think this would be an interesting point given recent work has focused on the role of orographic drag in improving the simulation of blocking (Pithan et al. 2016 GRL) and zonally asymmetric boundary conditions have been hypothesised to be critical for blocking formation (e.g., Tung and Lindzen 1979). Moreover, the results suggest that the poor simulation of blocking in climate models for the past several decades (e.g., Davini and D'Andrea 2016 JCLIM) could be better understood by understanding blocking dynamics in more simple aquaplanet models.

[Ans] We acknowledge the constructiveness of this comment and have made changes to the focus and set of orographic configurations for this study. For our research questions we now focus on analyzing how realistic blocks in the aquaplanet are (this result is further emphasized in the revised block centered compositing analysis (Fig. 3 section 3.1), and how the spatial distribution and duration of blocking responds to mountains.

In response to your suggestion of using simpler models, we now primarily focus on single mountain integration of varying height, rather than various configurations with multiple mountains as before. We also now cite have included the work of Pithan et al. as a reference in the discussion section, see lines 459-460:

"This configuration is like the others that include mountains in that it imposes zonally asymmetric forcing in land-sea contrast and orographic drag (Pithan et al., 2016)"

Given this different perspective and the issues discussed in general comment 1, a suggestion to improve the paper would be to focus on the following questions:

1) Are the characteristics of individual blocking events different with zonally symmetric versus asymmetric boundary conditions?

2) do zonally asymmetric boundary conditions control the spatial statistics of blocking?

3) Are the hemispherically integrated statistics of blocking different for zonally symmetric versus asymmetric boundary conditions?

[Ans] Thank you for the suggestions. We have incorporated them into the formulation of the questions being addressed in the revised version of this paper. The questions are restated below:

1. Are blocks in an aquaplanet dynamically similar to blocks in orographically forced simulations and reanalysis?
2. Does the presence of orography affect the overall frequency of blocking?
3. How does orography affect the spatial distribution of blocking frequency?
4. Does orography affect the duration of blocking events?

Specific comments:

1. *Lines 18-19: This suggests high-latitude blocking is different from reanalysis in the model however the text says the opposite.*

   [Ans] These lines from the abstract are removed as well as the related analysis from the manuscript.

2. *Lines 42-43: Is this true if you integrate blocking statistics over the entire NH versus SH? How different are the statistics quantitatively?*

   [Ans] Yes this holds when you integrate blocking statistics over the NH and SH. This is discussed quantitatively in results section 3.2.2, lines 350-351:

   "For the NH (SH) in this dataset, 485 (336) blocking events are found yielding a hemispherically-averaged blocking frequency of 2.7 % (1.6 %)."

3. *Line 46: I think a better topic sentence for this paragraph is that the dynamics of blocking are unclear. Also I suggest to cite Nakamura et al. (2018) Science. Their work provides a simple theory for which can be used to explain why stationary waves preferentially localise blocking in certain longitudes, e.g., they slow the 'speed limit' and modify the source of zonal wave activity flux.*

   [Ans] The original topic sentence is removed; this paragraph now begins with a discussion of the theories behind blocking explicitly. Nakamura and Huang (2018) is now more explicitly referenced through the paper, especially in regard to enhanced blocking found near the high-pressure stationary wave anomaly. The new version of this paragraph can be found in lines 64-70:

   "Previous work suggests that the spatial distribution of blocking frequency (hereafter, the blocking climatology) is dependent on the behaviour of the stationary waves, jet streams, and storm tracks. Nakamura and Huang (2018) for example, propose that blocking is most ubiquitous in regions where the positive anomaly in the stationary wave maximizes, and mean westerly flow is weak. Work by others on the effects of transient eddy forcing on blocks (Shutts, 1983; Nakamura et al., 1997; Takaya and Nakamura, 2001; Wang and Kuang, 2019), shows the importance of the storm tracks. The work presented here aims to better characterize the manner in which the spatial distribution of the stationary waves, jet streams, and storm tracks are linked to the blocking climatology."

4. *Lines 72-74: Suggest adding 'in order to relate the idealized results to the real atmosphere, e.g. NH vs SH and NH PAC vs NH ATL'.*

   [Ans] This part of the introduction has been revised to align with the overall updates.

5. *Line 94: Does the omission of these processes influence blocking in the model compared to the real world? e.g. diabatic effects shown by Pfahl et al. (2015) nature.*

[Ans] According to the work of Pfahl et al (2014)., Steinfeld et al. (2019), etc., the omission of diabatic processes certainly should have an influence on blocking. This model does include latent heat release due to the condensation of water vapor, both in the large scale and parameterized sense. The main simplification is that it does not include the impacts of clouds. See Frierson et al., 2006, JAS for more details on the model.

6. *Line 96: The experiments include both topography and land-sea contrast, yet the title only mentioned topography. What is more important for the results, topography or land-sea contrast?*

   [Ans] We have updated the title to eliminate this ambiguity. We replace “topography” with “orography” to encompass changes in both land-sea contrast and lower boundary height. This is a great question, but beyond the scope of this work. With the orographic configurations used here, we cannot answer this question, however we do partially examine this topic in the discussion section where we present results from a run with a flat land patch.

7. *Line 99: Suggest mentioning again why this specific configuration is used: to relate results to the real atmosphere.*

   [Ans] Explicit reminder is now included in line Section 2.2, lines 109-111:

   “TwoMtn: 1 integration with two Asymmetrically placed 3 km high Gaussian mountains centered at 45° N, 90° E and 45° N, 150° W, respectively. This placement is to loosely mimic the wide (Pacific) and short (Atlantic) zonal extents of the NH ocean basins.”

8. *Lines 100-106: Have the authors confirmed how their results are sensitive to the mountain amplitude?*

   [Ans] This is investigated in the new set of model configurations with topography, Fig. 6, Section 3.2.3.

9. *Section 2.3: Could the anomaly normalisation or the spatial area threshold used to identify events be responsible for the different blocking events in mid versus high latitudes? Longitude lines converge poleward and the thresholds were likely tuned for midlatitudes. Have the authors checked the sensitivity of their results do different thresholds? Or a different blocking index? I suggest confirming the results with a simpler index involving only geopotential height anomalies or the reversal of the geopotential.*

   [Ans] To mitigate any discrepancies related to this, we have removed the section of this paper analyzing midlatitude vs high-latitude blocking episodes. Regarding sensitivities in the blocking index, it proved impractical to implement and analyze different indices. This index however has proven be reliable, and our results are similar to that of previous work.

10. *Sections 2.4.1-2.4.2: I suggest mentioning this in words in the results instead.*

[Ans] We acknowledge this criticism but choose to maintain this structuring to provide quick, localized references of these analysis metrics for the reader. To condense things, we have combined the explanation of the stationary wave and storm track into one subsection (2.4.1), and the blocking and zonal wind climatologies into another (2.4.2). These fields are grouped together in a consistent way in which they are presented in Figure 4-7, and 9.

11. Section 2.4.3: Isn't a simple lanczos filter more commonly used (e.g. Shaw et al. 2016 nature)?

[Ans] In our experience, there are many different acceptable methods for filtering the data to isolate the transient eddies used in the calculation of the storm tracks. The Wallace et al. 1988 paper makes a point of explaining how the 24-hour differences of the daily means acts to filter the data in a similar manner to a bandpass filter (using a technique such as the Lanczos filter). The review of storm tracks by Chang et al. (2002, J. Climate) gives a brief history of the subject of time filtering. Guo et al. (2009) use the same filtering method as we use here, because they work with observational data that is only available as daily samples, this, we think offers one advantage of the 24-hour differencing method. Another advantage is that the 24-hour difference algorithm could be coded into GCMs in a manner that would allow the models to calculate the storm tracks online, to create climatological statistics, without saving a large amount of high-frequency temporal data.

12. Section 2.4.5: I'm confused about the wave activity flux vectors. Shouldn't these be calculated for high-frequency eddies only since they characterize their influence on low-frequency blocking? e.g., Hoskins et al. 1983 JAS Fig. 15. Here the quantities used to calculate the fluxes are low pass filtered.

[Ans] Hoskins et al. 1983 JAS formulates a quantity designated as the E-Vector. It can be thought of as the effective easterly momentum flux, where converging E-Vectors corresponds to a suppression of westerly mean flow, and thus the negative forcing of the eddies on the mean state. Hoskins et al. presents the E-vector for both low frequency (7-day lowpass) and high-frequency (7-day high pass) eddies computed with respect to the climatological mean.

In this work, the wave activity flux formulated by Takaya and Nakamura 2001 is utilized. In Takaya and Nakamura 2001 and Nakamura et al. 1997, wave activity fluxes are calculated as 8 day low-pass filtered eddies with the climatologies of the relevant input fields removed. The wave activity flux also relates eddy feedback onto the mean state, but by definition, is the pseudo-momentum associated with Rossby Waves. Both the E-vector and wave activity flux have proven to be useful, and the differences are subtle, but one advantage of the wave activity flux is that it is an instantaneous quantity.

In the original manuscript analysis, the stationary term of the wave activity flux was computed using 3 to 30 day bandpass, and 30-day lowpass filters to calculate the eddy and mean states, respectively. The formulation of wave activity flux in Takaya and Nakamura 2001, however, includes a non-stationary term that contributes much more in the high frequency regime. Therefore, to minimize the non-stationary influence of wave activity flux, our analysis now instead focuses on wave activity fluxes of low frequency eddies calculated using an 8 to 30 day bandpass on the input fields. We have updated Section 2.4.3, lines 184-190, to be clearer:

“To better characterize the dynamical evolution of blocks within each model, wave activity flux vectors (hereinafter, $\vec{\boldsymbol{W}}$) are calculated as described by Takaya and Nakamura (2001), hereinafter TN01. The wave activity flux relates eddy feedback onto the mean state and is essentially the pseudo-momentum associated with Rossby waves. Convergence of $\vec{\boldsymbol{W}}$ is associated with blocking and an overall slowing or reversal of westerly flow. The formulation of $\vec{\boldsymbol{W}}$ in TN01, includes a stationary term that dominates for quasi-stationary, low frequency eddies (i.e. 8- to 30-day timescales), and a non-stationary, group-velocity dependent term that is more relevant for higher frequency eddies. Here we calculate only the stationary, horizontal component of $\vec{\boldsymbol{W}}$, and focus on contributions solely from the low frequency eddies.”

13. *Lines 247-248: I suspect that the lower statistical significance threshold was used because the blocking statistics are not that different between the zonally symmetric versus asymmetric experiments. This supports general comment 3 above.*

[Ans] We received similar feedback in the other reviews. After further self-clarification we have now chosen a 95% confidence interval and more careful wording to describe quantitative differences throughout our analyses. See the methods subsection 2.5.4, lines 256-257:

“A 95% confidence interval is imposed as the significance threshold for all significance testing.”

14. *Lines 290-291: I disagree. The contours differ by 25m, e.g. 275 versus 300.*

[Ans] This analysis is now removed.

15. *Lines 505-506: I believe Hassanzadeh et al. 2014 used a dry-dynamical core not an aquaplanet model.*

[Ans] We have updated any reference to this work to not refer to it as using an aquaplanet. Instead we use “idealized model with zonally symmetric forcing”.

16. *Lines 537 and 545: Resonance has a very specific meaning, e.g., multiple reflection of waves on turning points following linear theory. I don't think it is what is implied here.*

[Ans] Agreed, this is removed.

17. *Figs 2,3,4 and 9 and related analysis: I suggest the authors interpret the wave activity fluxes with regards to flux convergence not the flux itself since this is the key dynamical quantity for blocking (Hoskins et al. 1983 JAS, Nakamura et al. 2018 science).*

[Ans] Agreed, this is now presented in Fig. 3 of the revised manuscript.

18. *Figs. 3 and related analysis: I suggest the authors compare the zonally-symmetric and asymmetric model simulations with reanalysis explicitly rather than reference previous work. Specifically, I suggest replacing Fig. 3 with a 3 x 3 panelled figure showing midlatitude blocking for reanalysis (top), zonally symmetric model (middle) and one zonally asymmetric model simulation for all 3 lifecycle stages (left, middle, right). This would also show that the two model configuration show similar results.*

[Ans] Agreed, see Fig. 3 and section 3.1.

Response to Reviewer 3

The authors have used an idealized moist GCM and investigated some of the spatial and temporal characteristics of blocking events in the absence and in the presence of topography. I find the objectives of the paper and its results interesting and important (although further clarifications are needed). The paper is well structured and well written. I have a number of major and minor comments, which are listed below.

[Ans] Thank you for the feedback. As discussed in the cover letter we have adjusted the article to focus more on the results from the aquaplanet, comparing them to results from reanalysis and idealized model integrations with topography.

Recommendation: major revision
Major comments My major concern is that the paper is focused on too many questions, which have made the answers sometimes a bit too speculative. It appears to me that the three main questions are

1- *Do the blocking events in aquaplanet simulations have the same dynamics as those of the real blocking events? This is a great question and its answer has important implications for our understanding of the dynamics of the blocking events, as for example, some blocking theories require zonal asymmetries in boundary conditions/forcings. The studies of Hu et al. (2008 GRL), Hassanzadeh et al. (2014 GRL), and more recently Nabizadeh et al. (2019 GRL) have shown the existence of blocking events in aquaplanet simulations and report some of their characteristics, but certainly, there is a need for further investigation, and I am glad that these authors have focused on this question. Given the importance of the answer, I believe that the statement in Lines 296-298 needs more support. To start, I suggest that you show the analysis of Fig. 3 for the ERA data as well, so that the readers can see the comparison side by side (rather than being referred to other papers such as TN01).*

   [Ans] This feedback led to a greater emphasis on the aquaplanet results and the reformulation of research question 1 (see last bullet point of Major Changes section of this document). We now include citations for Nabizadeh et al. 2019 GRL anywhere we discuss previous results from idealized models with zonally symmetric forcing. Fig. 3 now shows a side by side comparison of the dynamical evolution of blocking events in the aquaplanet, topographic configurations, and reanalysis. Reviewer 2 also had similar thoughts

2- *Do the high-latitude blocks have the same dynamics as those of the midlatitude blocking events? The discussion in lines 286-292 is too speculative. I suggest that you show the analysis of Fig. 3 but for high latitude blocks (rather than the single panel in Fig. 4). Regarding the difference in dynamics: given the lack of W and weakness of the anomalies (pointed out in lines 290-291), is it possible that the high-latitude blocks are just cut-off highs that appear stationary because the zonal wind in the high latitudes is weak? (so there is really no maintenance mechanism?) What is the time scale of zonal advection in the high latitudes of the models (and what is it in the midlatitudes?)*

[Ans] To avoid issues and ambiguities related to midlatitude vs. high-latitude blocking, and based on a comment from reviewer 2, we have chosen to remove this section entirely from the manuscript. Perhaps this will be a focus of future work.

3- *What is the effect of topography on the duration, distribution, and dynamics? I think here the most interesting analysis is the comparison between Fig. 3 and 9. Whether the life cycle and dynamics are affected by the topography or not is an important question but is barely explored. I suggest that you further elaborate on these results. Otherwise, given the very idealized nature of topography here, I am not sure how much we can learn from the distribution and duration of different simulations with different topography configurations.*

[Ans] As mentioned above, Fig. 3 now includes a side-by-side comparison of blocks in the aquaplanet with blocks from the topographic configurations. The result remains the same.

With regards to duration, the revised manuscript provides better framing for the duration analysis, particularly in Section 3.2.4, lines 402-404 leading into the block duration analysis:

“The TwoMtn configuration has a greater hemispherically averaged blocking frequency than the other configurations (Table 2). This is despite the TwoMtn configuration having a lower total number of blocks than the 3 and 4 km SingleMtn configurations, respectively – meaning the blocks have a longer average duration in the 2-mountain configuration.”

We still find the suggested increase in block duration for blocks forming near topography to be an interesting piece of the story. A natural question from the climatology analysis is: Do more events or longer lasting blocks cause the overall increase in hemispherically averaged blocking statistics within the idealized model integrations with topography compared to the aquaplanet? These results provide insight into this question, showing that it is a complex mixture of both. Differences in duration found in this study, albeit sometimes modest, also are consistent with popular theories linking a high propensity of blocking to weak zonal background flow (i.e. Nakamura and Huang 2018 science).

Minor comments
L186: W is given in : : :..

[Ans] Typo corrected, colon corrected.

L247: 85% is too low. I suggest using a 95% confidence interval.

[Ans] We received similar feedback in the other reviews. After further self-clarification we have now chosen a 95% confidence interval and more careful wording to describe quantitative differences throughout our analyses. See the methods subsection 2.5.4, lines 256-257:

“A 95% confidence interval is imposed as the significance threshold for all significance testing.”

Atmospheric Blocking in an Aquaplanet and the~~: The~~ Impact of Orography~~Topography in an Idealized General Circulation Model~~

Veeshan Narinesingh[1,2], James F. Booth[1,2], Spencer K. Clark[3], Yi Ming[4]

[1]Department of Physics, City University of New York – The Graduate Center, New York, New York, 10016, United States of America

[2]Department of Earth and Atmospheric Sciences and NOAA-CESSRST, City University of New York – City College, New York, New York, 10031, United States of America

[3]Program in Atmospheric and Oceanic Sciences, Princeton University, Princeton, New Jersey, 08544, United States of America

4 Atmospheric Physics Division, NOAA Geophysical Fluid Dynamics Laboratory, Princeton, New Jersey, 08540, United States of America

Correspondence to: Veeshan Narinesingh (veenarinesingh@gmail.com)

Abstract.

This work utilizes an idealized moist GCM to investigate~~Atmospheric blocking can have important impacts on weather hazards, but the fundamental dynamics of blocking are not yet fully understood. As such, this work investigates the influence of topography on~~ atmospheric blocking in terms of dynamics, spatial frequency, and duration. The model is first configured as ~~and displacement. Using an idealized GCM,~~ an aquaplanet, then orography is added in separate ~~integration, and~~ integrations ~~with topography are analyzed~~. Block-centered composites of wave activity fluxes and height show that blocks in the ~~midlatitude~~ aquaplanet undergo a realistic dynamical evolution when compared to reanalysis. Blocks in the aquaplanet are also found to have ~~blocks exhibit~~ similar lifecycles to blocks in model integrations with orography. These results affirm the usefulness of both zonally symmetric and asymmetric idealized model configurations for studying blocking. Adding orography to the model leads to an increase in blocking. This mirrors what is~~wave activity flux behavior to those~~ observed when comparing the northern (NH) and southern hemispheres (SH)~~in reality, whereas high-latitude blocks do not. The addition~~ of Earth, where the NH contains more orography, and thus more~~topography significantly increases~~ blocking. As the prescribed mountain height is increased, so does the magnitude and size of climatological stationary waves, resulting in more blocking overall. Increases in blocking however, are not spatially uniform. Orography is found to induce ~~and determines distinct~~ regions of enhanced block frequency just upstream of mountains, ~~where blocks are most likely to occur. These regions are found~~ near high ~~-~~pressure anomalies in the stationary waves which is poleward of climatological minima in upper level zonal wind. While block frequency minima and jet maxima occur eastward of the wave trough. This result matches what is observed ~~and~~ near the Rocky Mountains. Finally, an analysis of~~storm track exit regions. Focusing on~~ block duration shows~~,~~ blocks generated~~originating~~ near stationary wave maxima~~topography are found to~~ last slightly longer than blocks~~those~~ that form~~are formed without or~~ far from, or without orography ~~topography but have qualitatively similar evolutions in terms of nearby geopotential height anomalies and wave activity fluxes in composites. Integrations with two mountains have greater amounts of blocking compared to the single mountain case, however, the longitudinal spacing between the mountains is important for how much blocking occurs. Comparison between integrations with longitudinally long and short ocean basins show that more blocking occurs when storm track exits spatially overlap with high-pressure maxima in stationary waves. These results have real-world implications, as they help explain the differences in blocking between the Northern and Southern Hemisphere, and the differences between the Pacific and Atlantic regions in the Northern Hemisphere~~.

1 Introduction

Atmospheric blocks are quasi-stationary anticyclones that can cause temperature extremes (Sillman et al., 2011; Pfahl and Wernli, 2012), steer hurricanes and extratropical cyclones (Mattingly et al., 2015; Booth et al. 2017, respectively), and induce persistent weather (Cassou et al., 2005; Dole et al., 2011; Brunner et al., 2018). Despite the expensive and sometimes deadly impacts of blocks, many fundamental questions remain regarding their behaviour~~behavior~~, and models tend to underpredict blocks in terms of their frequency and duration (D'andrea et al., 1998; Matsueda, 2009). ~~Wintertime blocks are particularly interesting, because they occur during the season when the jet stream and extratropical cyclones are strongest.~~ As such, this paper utilizes an idealized general circulation model~~seeks~~ to expand our understanding of ~~wintertime~~ blocks, focusing on the representation in models configured with and without mountains.~~their dynamics, spatial distribution, frequency, duration, and displacement.~~

~~The climatological spatial distribution of blocks is well documented.~~ ~~In Winter for the Northern Hemisphere, two main regions of blocking occur at the north-eastern edges of the Atlantic and Pacific Ocean basins (Barriopedro et al., 2006; Croci-Maspoli et al., 2007; Dunn-Sigouin et al., 2013). In the Southern Hemisphere (SH), one main region of blocking exists, located southwest of South America (Renwick, 2005; Parsons et al., 2016; Brunner and Steiner, 2017). Overall, blocking occurs more frequently in the Northern Hemisphere (NH) than the Southern. This difference in blocking frequency is likely related to the stronger stationary wave in the NH, often attributed to more prominent midlatitude topography and land-sea contrasts in the NH, e.g., Held et al. (2002). However, to our knowledge, no study has confirmed this assumption.~~

~~Why blocks preferentially occur in certain regions remains unclear.~~ Some have argued that blocks are consequences of an interaction between eddies and stationary waves induced by orography (Egger, 1978; Charney and Devore, 1979; Tung and Lindzen, 1979; Luo, 2005). These studies suggest mountains are critical for the overall existence of blocking and setting the location of climatological block frequency maxima. On the other hand, Shutts (1983) used a barotropic~~uses an idealized~~ model to show that blocking flows do not necessarily need stationary forcing and can arise purely through interactions between transient eddies. Confirming this, Hu et al. (2008), Hassanzadeh et al. (2014), and Nabizadeh et al. (2019) have more recently shown that blocks do indeed occur in idealized models in the absence of zonally asymmetric forcing.

This suggests the extratropical cyclones (i.e., synoptic-scale eddies) that occur upstream of the blocking regions may be key. ~~Related to this~~ Colucci (1985) and Pfahl et al. (2015) show that extratropical cyclones can impact blocks downstream of the storm track exit region. In a related theory, blocks are linked to Rossby wave-breaking (Pelly and Hoskins, 2003; Berrisford et al.,~~,~~ 2007; Masato et al., 2012), which primarily~~and wave-breaking~~ occurs in ~~more frequently at the storm track exit~~ regions~~. Thus, for the NH, there are two factors that might have important roles in determining the characteristics~~ of weak westerly flow~~blocking: the topographically induced stationary waves and the storm track exit regions~~.

~~The proposed factors that may influence blocking in the NH, make the presence of blocking in the SH all the more interesting. Most SH blocks occur at higher latitudes than the NH counterparts, and have less impact on the zonal flow (Berrisford et al., 2007).~~ Hu. et al. (2008) presents case studies that show blocks in an aquaplanet model behave in a realistic manner. They also~~However, blocks can occur throughout the SH storm track region, far from topography. Related to this Hu~~

~~et al. (2008) and Hassanzadeh et al. (2014) show blocks can occur in idealized aquaplanet configurations. Hu et al. (2008)~~ find that blocks in their aquaplanet model occur more frequently than what is observed in nature – regardless of hemisphere, which is contradictory to the idea that stationary waves facilitate blocking episodes. The results of Hu et al. (2008) however, are complicated by known discrepancies within the community regarding the identification ~~of blocks~~ (e.g. Barnes et al., 2012) and seasonality (Barriopedro et al., 2010) of blocking. In Hu et al. (2008),~~), where they compare their idealized model~~ results from their perpetual equinox aquaplanet are compared to Weidenmann et al. (2002), who use a different~~study that uses an alternate~~ block identification algorithm~~metric~~ on reanalysis over all seasons.~~data.~~ Thus, questions remain regarding the relative~~relatively~~ frequency of blocks with and without the presence of mountains.~~topography.~~

~~The work herein focuses on climatological and dynamical aspects of atmospheric blocks using an idealized moist GCM. The first analysis focuses on blocks in an aquaplanet configuration. For this, we present composites of the evolution of geopotential height anomalies and wave activity flux throughout block lifecycles and compare midlatitude and high-latitude blocking. For the second analysis, we start by studying the climatological flow features and block spatial frequencies in reanalysis as a benchmark. We then add topography to the aquaplanet and examine the response of climatological flow features and block spatial frequency. We adjust the number and placement of the topographic features so that we can determine the response of blocking to topography, the storm tracks, and the distance between the two features, i.e., the zonal extent of the ocean basins between the topographical features. Finally, the third analysis examines the sensitivity of block duration and displacement for the different topographical configurations.~~

The climatological spatial distribution of blocks is well documented. In the cool months of the Northern Hemisphere (NH), two main regions of blocking occur at the north-eastern edges of the Atlantic and Pacific Ocean basins (Barriopedro et al., 2006; Croci-Maspoli et al., 2007; Dunn-Sigouin et al., 2013). In the Southern Hemisphere (SH), one main region of blocking exists, located southwest of South America (Renwick, 2005; Parsons et al., 2016; Brunner and Steiner, 2017). Overall, blocking occurs more frequently in the northern hemisphere than the southern. This difference in blocking frequency is assumed to related to the stronger stationary wave in the NH (Nakamura and Huang, 2018), often attributed to more prominent midlatitude topography and land-sea contrasts, e.g., Held et al. (2002). However, to our knowledge, no study has confirmed this assumption.

Previous work suggests that the spatial distribution of blocking frequency (hereafter, the blocking climatology) is dependent on the behaviour of the stationary waves, jet streams, and storm tracks. Nakamura and Huang (2018) for example, propose that blocking is most ubiquitous in regions where the positive anomaly in the stationary wave maximizes, and mean westerly flow is weak. Work by others on the effects of transient eddy forcing on blocks (Shutts, 1983; Nakamura et al., 1997; Takaya and Nakamura, 2001; Wang and Kuang, 2019), shows the importance of the storm tracks. The work presented here aims to better characterize the manner in which the spatial distribution of the stationary waves, jet streams, and storm tracks are linked to the blocking climatology.

This article focuses on 4 main research questions:

4

1. Are blocks in an aquaplanet dynamically similar to blocks in orographically forced simulations and reanalysis?
2. Does the presence of orography affect the overall frequency of blocking?
3. How does orography affect the spatial distribution of blocking frequency?
4. Does orography affect the duration of blocking events?

To address question 1, we use compositing analysis to compare the life cycles of blocks for an aquaplanet, reanalysis and a model with orography. For questions 2 and 3, we compare the climatology of blocking, stationary waves, jet streams, and storm tracks for models with different orographic configurations. To answer question 4, we carry out an analysis that examines the sensitivity of block duration to mountains.

2 Methods

2.1 Reanalysis data

Although the focus of this paper is on ~~a set of~~ idealized numerical modelling experiments, we also~~first~~ present results using reanalysis to motivate our work. The reanalysis used is the ECMWF ERA-Interim dataset (Dee et al., 2011). ERA-Interim (ERAI) has been shown to represent winter midlatitude storms as well as, and in some cases better than, other reanalyses (Hodges et al., 2011). Therefore, it likely does a reasonable job at capturing atmospheric blocking. ERA-Interim is produced using a model with roughly 0.67-degree resolution, but it is available to download at different resolutions. Herein, we used data with a 1.5 x 1.5 degree horizontal resolution. For this analysis we focus only on the cool season from 1979-2017~~winter~~, which is defined as Nov. – Mar.,~~Dec. – Feb. (DJF)~~ and May – Sept.~~Jun. – Aug. (JJA)~~ for the Northern and Southern Hemispheres, respectively. Blocks are most abundant during these months (Tibaldi et al., 1994; Barriopedro et al., 2010).

2.2 Idealized model configuration

This work utilizes an idealized moist GCM described by Clark et al. (2018; 2019), which is modified from that introduced by Frierson et. al. (2006; 2007) and later altered by Frierson (2007) and O'Gorman and Schneider (2008). The model is configured to use 30 unevenly spaced vertical sigma coordinate levels, and T42 spectral resolution, corresponding to 64 latitude by 128 longitude grid points when transformed to a latitude-longitude grid. Earth-like orbital parameters are used to simulate a full seasonal cycle in solar insolation. The model includes full radiative transfer and simplified physics parameterizations of convection (Frierson, 2007), boundary layer turbulence (Troen and Mahrt, 1986), and surface fluxes. There is no treatment of cloud radiative effects or condensed water in the atmosphere.

An aquaplanet configuration is run as the control integration. For the~~In other~~ integrations with mountains, configurations of topographical forcing are simulated by modifying the model surface height and using a simplified treatment of land following Geen et al. (2017) and Vallis et al. (2018). Like Cook and Held (1992), and following Lutsko and Held (2016), perturbations to the surface height are introduced in the form of Gaussian mountains centered at 45° N with half-widths

~~5~~

of 15 degrees in both the latitude and longitude dimensions. Several configurations are examined in this work~~Here, mountains are placed in various zonal configurations for the topographic integrations (Figure 1). The 4 configurations are~~:

a) Aquaplanet: idealized model with no orography

~~b)~~ SingleMtn: **4 separate integrations with a single**~~Single 3 km high~~ Gaussian mountain centered at 45° N, 90° E **of variable peak height (1 km, 2**~~.~~

~~c)~~**b)** ~~SymMtn: Two Symmetrically placed 3~~ km, 3 km, 4 km~~ high Gaussian mountains centered at 45° N, 90° E and 45° N, 90° W~~ respectively)~~.~~

~~d)~~**c)**TwoMtn: 1 integration with two~~AsymMtn: Two~~ Asymmetrically placed 3 km high Gaussian mountains centered at 45° N, 90° E and 45° N, 150° W respectively. This placement is to loosely mimic the wide (Pacific) and short (Atlantic) zonal extents of the NH ocean basins.

The 3 km SingleMtn and TwoMtn configurations are shown in Figure 1. Ocean grid cells are represented using~~contain~~ a ~~20 m~~ slab ocean with~~, and as~~ a depth of 20 m. For simplicity~~simplification, are assumed to redistribute zero energy horizontally; that is,~~ we prescribe uniformly zero ~~heat flux, often referred to as a~~ Q-flux, meaning that we assume that in the time mean, the net flux of energy from ~~into or out of~~ the ocean to the atmosphere is zero at all surface grid cells.~~.~~ In the configurations with mountains~~topography~~, land grid cells are defined as locations where the height is greater than 1/100th of the maximum surface height (3 km), corresponding to a height threshold of 30 m. As in Geen et al. (2017) and Vallis et al. (2018) land is simulated by reducing the slab ocean depth to 2 m (effectively reducing the heat capacity) and limiting evaporation using a bucket hydrology model. A uniform surface albedo of 0.26 is used to obtain a global annual mean surface temperature resembling that of the Earth. Each configuration is integrated for 40 years, but the first 10 years are discarded as spin-up time. Thus, the results presented here are for years 11-40 of each integration. 6-hourly data sets are used for the analyses in this paper, and the results are presented for Northern Hemisphere cool season~~Winter~~, defined as the 5~~3~~ months centered on the minimum in solar insolation. The model data is interpolated to the 1.5 x 1.5 degree horizontal ERA-Interim resolution prior to any analysis.

2.3 Block detection and tracking

Here we use a 500 hPa geopotential height (Z500) hybrid metric that utilizes the Z500 anomaly and meridional gradient. This metric was chosen for its robustness~~–~~ in terms of capturing high amplitude events involving wave-breaking (Dunn-Sigouin et al., 2013), and because it only requires the Z500 field – which simplifies tracking when analyzing large datasets. Barnes et al. (2012) finds that utilizing a Z500 metric produces similar blocking durations and climatologies to both potential vorticity and potential temperature based metrics. Blocks are detected and tracked using the algorithm described by Dunn-Sigouin et. al. (2013), hereinafter as DS13, which is an adaptation of previous methods by Barriopedro et al. (2010) and Sausen et al. (1995). This algorithm searches for large, contiguous regions of persistent, high amplitude, positive anomalies in the Z500 field. Within these regions, ~~the~~ Z500 must satisfy a meridional gradient reversal condition. What follows is an overview of the block identification algorithm, but specific details can be found in DS13:

1. Z500 Anomaly Calculation: For each grid-point poleward of 30 N, from the raw Z500 field subtract the running annual mean and mean seasonal cycle as computed in DS13.

2. Normalize each anomaly value by the sin of its latitude divided by sin of 45 degrees, i.e. $\frac{sin(\phi_{ij})}{sin(45°)}$, $\cancel{\frac{\sin(\phi_{ij})}{\sin(45°)}}$, where ϕ_{ij} is the latitude of an arbitrary grid-point with longitude *i* and latitude *j*. This normalized anomaly will be referred to as Z500'.

3. For each month, in a 3-month window centered on a given month, calculate the standard deviation, S, of all Z500' values.

4. Amplitude threshold: Identify contiguous regions of positive Z500' greater or equal to 1.5*S.

5. Size threshold: Regions must be at least 2.5 x 10^6 km^2 in area.

6. Gradient Reversal: The meridional gradient of the Z500 field within candidate regions must undergo a reversal in sign as described by DS13.

7. Quasi-stationary condition: For each timestep, regions must have a 50 % area overlap with its previous timestep (modified from DS13's 2 day overlap which was applied to daily mean data)

8. Blocks must meet the above criteria for at least 5 days (e.g. 20 6-hourly timesteps)

In case studies using ERAI and the idealized configurations described here, it was observed that two existing blocks sometimes merged with one another to form a single, larger block. We objectively identified this merging process based on extreme shifts in the location of the block centroid (defined as the gridpoint that is the centroid of the anomalous area associated with the block). If the centroid shifted by more than 1500 km from one 6-hourly snapshot to the next, we labelled~~labeled~~ the block as a merged event. These merged events represented 23-27 percent of the total initial blocks found in the idealized model integrations.~~four configurations.~~ We judge these events to be unique in terms of their relationship between block duration. Furthermore, the merger-blocks create uncertainty in terms of defining a block centre~~center~~ for the sake of our block-centered composite analysis. Therefore, we have excluded the merged events from our block-centered compositing and block duration analyses. The blocking climatological analysis on the other hand, retains all blocks since the primary focus is on the spatial distribution of block frequency, not the individual blocks themselves~~analysis, and plan future work focused on these merged-block events~~.

2.4 Analysis metrics

The metrics used to characterize climatological features and blocking in the idealized model data and reanalysis are outlined below.

2.4.1 Stationary Wave and Eulerian Storm Track~~wave~~

The cool season~~winter~~ stationary wave at each point is defined as the anomaly with respect to the zonal mean of the cool season~~winter~~ climatology for the 250-hPa geopotential height field: $\bar{Z}^* = \bar{Z} - \left[\bar{Z}\right]$, where brackets indicate the zonal mean and overbar indicates the time mean over cool season~~winter~~ days for all years. This is computed separately for each gridpoint.

The Eulerian

~~**2.4.2 250 hPa zonal wind climatology**~~

~~The 250 hPa zonal wind climatology (U250) is presented as the time mean of the 250-hPa zonal wind over the winter months at each gridpoint.~~

~~**2.4.3 Eulerian storm track**~~

~~The~~ storm track is presented as the standard deviation of a 24-hour difference of the daily mean Z500 field during cool season~~winter~~ (Wallace et al.,~~all.~~ 1988; Guo et al., 2009; Booth et al., 2017). Consider $Z_{500}(t)$ to be the daily mean Z500 value for an arbitrary gridpoint. To obtain the storm track:

1. The 24-hour difference, Z_{500}^{τ}, at each gridpoint is taken as:

$$Z_{500}^{\tau} = Z_{500}(t+1) - Z_{500}(t)$$

2. Then, the standard deviation of Z_{500}^{τ} for all cool season~~winter~~ timesteps at each gridpoint is taken to obtain the cool season~~winter~~ Eulerian storm track value at that point.

This is computed separately for each gridpoint.

2.4.2~~4~~ Blocking and Zonal Wind Climatologies~~climatology~~

The spatial distributions of blocking frequency, referred to hereinafter as the blocking~~Blocking~~ climatologies, are calculated by averaging the block identification flag (1 or 0 respectively) per gridpoint over all cool season~~winter~~ days. Thus, the blocking climatologies show the percent of cool season~~winter~~ timesteps a block (as defined here) is present. This is computed separately at each gridpoint.

The 250 hPa zonal wind climatology, hereinafter referred to as $\overline{U250}$, is presented as the time mean of the 250-hPa zonal wind over the cool season months at each gridpoint.

~~8~~

2.4.3~~5~~ Wave activity flux vectors

To better characterize the dynamical evolution of blocks within each model, wave activity flux vectors (hereinafter, $\vec{\boldsymbol{W}}$) are calculated as described by Takaya and Nakamura (2001), hereinafter TN01. The wave activity flux relates eddy feedback onto the mean state and is essentially the pseudo-momentum associated with Rossby waves. Convergence of $\vec{\boldsymbol{W}}$ is associated with blocking and an overall slowing or reversal of westerly flow. The formulation of $\vec{\boldsymbol{W}}$ in TN01, includes a stationary term that dominates for quasi-stationary, low frequency eddies (i.e. 8- to 30-day timescales), and a non-stationary, group-velocity dependent term that is more relevant for higher frequency eddies. Here we calculate only the stationary, horizontal component of $\vec{\boldsymbol{W}}$, and focus on contributions solely from the low frequency eddies.

Block centered composites (as described in Sect. 2.5.1. of this paper) are ~~then~~ computed using $\vec{\boldsymbol{W}}$ for each block during various stages of the block's lifecycle. The horizontal components of $\vec{\boldsymbol{W}}$ are calculated as in TN01. For this, eddy fields are computed with an 8-~~only the stationary term was considered, which yielded similar results in reanalysis~~ to 30-day bandpass filter. This is what is described as low frequency eddies in ~~those presented in the original~~ TN01 and Nakamura et al. (1997).~~article.~~ $\vec{\boldsymbol{W}}$ are~~is~~ given by:

$$\vec{\boldsymbol{W}} = \frac{p\cos\phi}{2|\vec{U}|}\begin{pmatrix} U\left(v'^2 - \frac{\Phi'}{f}\frac{\partial v'}{\partial x}\right) + V\left(-u'v' + \frac{\Phi'}{f}\frac{\partial u'}{\partial x}\right) \\ U\left(-u'v' + \frac{\Phi'}{f}\frac{\partial v'}{\partial y}\right) + V\left(u'^2 + \frac{\Phi'}{f}\frac{\partial u'}{\partial y}\right) \end{pmatrix}$$

$$\cancel{\vec{\boldsymbol{W}} = \frac{p\cos\phi}{2|\vec{U}|}\left(\frac{U\left(v'^2 - \frac{\Phi'}{f}\frac{\partial v'}{\partial x}\right) + V\left(-u'v' + \frac{\Phi'}{f}\frac{\partial u'}{\partial x}\right)}{U\left(-u'v' + \frac{\Phi'}{f}\frac{\partial v'}{\partial y}\right) + V\left(u'^2 + \frac{\Phi'}{f}\frac{\partial u'}{\partial y}\right)}\right)}$$

This calculation is performed on variables on the 250-hPa pressure surface. For~~fields, where for~~ each point~~,~~ p is the pressure~~,~~ and ϕ is latitude. $\vec{U}$~~$\vec{U}$~~ is the 30-day low-pass filtered horizontal wind vector with zonal and meridional components U and V, respectively. The anomalous~~3-to-30-day bandpass filtered~~ zonal wind, meridional wind, and geopotential are given by u', v', ~~,~~and Φ~~Φ~~$'$, respectively. Derivatives are computed using finite-differencing, where zonal derivatives are weighted by latitude. $\vec{\boldsymbol{W}}$ are given in ~~units of~~ $m^2 s^{-2}$.

2.5 Analysis methods

2.5.1 Block-centered compositing

The Z500’, ~~field and~~ $\vec{W}$, and $\nabla \cdot \vec{W}$ fields are composited around the centroid of each block for the first, strongest, and final days of each block lifecycle ~~per run~~. To account for the convergence of meridians, relevant fields~~the Z500’ field and~~ ~~$\vec{W}$~~ are projected onto equal-area grids before compositing. The initial time step of a block is the first timestep that the block satisfies the amplitude, size, and reversal conditions. The strongest time step of a block is defined as the time step with the greatest Z500’ (at a single lat/lon location) within a block. The final timestep is the last timestep a block satisfies the amplitude, size, and reversal conditions.

The composites presented in this paper ~~for the aquaplanet, unless otherwise stated~~, only include midlatitude-blocks whose centroid are always south of 65° N. This is because we find that the high-latitude blocks exhibit distinct physical behaviour.~~behavior. The aquaplanet showed a greater tendency to produce more poleward blocks compared to the other configurations.~~ From reanalysis data, high-latitude blocks in the Southern Hemisphere have different dynamical evolution and different impacts on the surrounding flow, as compared to midlatitude blocks (Berrisford et al., 2007). The 65° N cut-off~~Based on these previous results and our own findings, we present separate results for the midlatitude (count = 95; see Sect. 3.1) and high-latitude blocks from the aquaplanet configuration (count = 46; see Sect. 3.2). The 65° N cutoff~~ was chosen after estimates showed this to be near the minimum in the meridional potential vorticity gradient, and thus the northern limit of the midlatitude waveguide (e.g. Wirth et al. 2018). Compositing results were robust to changes in cut-off latitude of +/- 7.5°~~After changing the cutoff by +/- 5°, 65° N proved to be the best compromise between distinguishing dynamical features between mid and high-latitude blocking, but also retaining enough members of each midlatitude and high-latitude subset~~.

2.5.2 Separating blocks by region

To compare the dynamical evolution of blocks originating near the eastern edge of the ocean basins (denoted as “East”, ~~,~~ near the windward side of mountains and the high-pressure maxima of stationary waves) against blocks originating elsewhere ~~near middle of the ocean~~ (denoted as “Other”),~~Mid, near the end of the storm tracks),~~ blocks are sorted by their centroid location during their first timestep. These regions are outlined in Table 1 and shown in Figure 1. The East region ~~Each region~~ spans 30°-65° N for 90~~100~~ degrees of longitude upstream and inclusive of the ~~. In SymMtn, we defined our East region relative to the~~ mountain centre.~~at 90E, which behaved similarly in our analyses to a region defined by the 90 W mountain instead.~~ For the TwoMtn~~AsymMtn~~ configuration, “East” and “Other”~~Mid~~ refer to two regions within the zonally larger ocean basin (which we refer to as the “Wide Basin”),~~wide basin),~~ whereas blocks originating within the zonally smaller~~other~~ ocean basin are ~~only~~ denoted as from the “Short Basin”. ~~by short basin. These regions are summarized in Table 1.~~

2.5.3 Block duration probability density distributions

Block duration is defined as the time interval from the initial identification timestep to the end of that block's existence – based on the block identification algorithm (described in Sect. 2.3). Each block is thus assigned one duration value. The steps taken to obtain block duration probability density distributions are as follows:

1. Sort blocks into subsets by model configuration and/or basin.
2. Allowing replacement, randomly select a set of block durations within a given subset. The size of the random set is given by the number of blocks in the subset being analysed~~analyzed~~.
3. Place the durations yielded by step 2 into n equal sized bins (n=8 for figures in this paper) ranging from the minimum to maximum duration of cool season~~winter~~ blocks between all model configurations.
4. Steps 2 and 3 are then repeated m times (m=1000 for figures in this paper) to produce an ensemble of m probability density distributions for each subset.
5. For a given subset, the mean probability density distribution is computed by taking the mean of that subset's distributions. This is then smoothed using a running mean.
6. For a given subset, the standard deviation of probability density distribution is computed by taking the standard deviation of that subset's distributions

The results of this paper are nearly constant with respect to changes in the values of n (+/- 2) and m (+/- 200). For all configurations, distributions and mean values presented for duration exclude any high-latitude blocking (blocks whose centroid are ever poleward of 65° N). 65° N was found to be the most appropriate cut-off in each configuration for the same reasons as described for the aquaplanet compositing.

2.5.4 Statistical significance ~~Block displacement~~

For a given gridpoint and cool season,~~To measure the propensity for individual blocks to move horizontally, we define~~ a block frequency value~~displacement metric. In this metric for an arbitrary block, the great circle distance between the block centroid at successive timesteps~~ is computed by averaging all the block identification flag values (1 or 0)~~. The block displacement~~ for each timestep~~block is the sum~~ of that cool season. This is done at every gridpoint for every cool season to yield a 3D matrix of dimensions latitude by longitude by ~~all displacements computed throughout its lifecycle, divided by the~~ number of years. ~~timesteps (i.e. the average centroid displacement every 6 hours).~~

2-sample t-tests are then performed for corresponding gridpoints.~~5.5 Statistical significance~~

~~To compare block frequency~~ between ~~configurations, the area-weighted mean of winter block frequency is computed for each year of~~ a given topographic configuration and a 250-year aquaplanet integration. A 250-year aquaplanet integration is used because the blocking climatology is more zonally symmetric when compared to climatology calculations that use less years. This is done to identify regions of enhanced and suppressed blocking frequency in the topographic integrations.

Significance testing in hemispherically averaged block frequency statistics are done by calculating area averaged blocking frequency for each cool season. For each configuration, this yields a one-dimensional array of values for each cool season.~~.~~ A 2-sample t-test is then used to examine ~~used on the yearly area-weighted mean values between configurations to test for~~ significant differences in hemispherically averaged block frequency between idealized model~~. Between~~ configurations. Significance~~ and regions, significance~~ testing for~~discerning~~ mean block duration also utilizes~~and displacement employ~~ a 2-sample t-test to compare differences between the various configurations and regions. A 95~~. An 85~~% confidence interval is imposed as the significance threshold for all significance testing.

3 Results

3.1 Blocking in the aquaplanet, dynamical aspects

On average, 12.9 blocks per cool season are identified for each hemisphere of the aquaplanet. The presence of blocking in this model configuration is consistent~~ According to our tracking algorithm, there are blocking events in the aquaplanet integration, which agrees~~ with previous studies that also find blocking in GCM's with zonally symmetric forcing~~idealized modeling work~~ (Hu et al., 2008; Hassanzadeh et al., 2014, Nabizadeh et al., 2019). ~~). An example of the beginning of a blocking episode in the aquaplanet can be seen in~~ Figure 2 shows a snapshot of the first day of an arbitrary block in the aquaplanet. Upstream and coincident with the block, a Rossby wave pattern can be observed in both the Z500 and Z500' fields (Fig. 2 - the Z500 contours show a wave-like feature, and the Z500' field shows an alternating pattern of low and high anomalies in the zonal direction). The presence of these features during the formation of a block agrees with previous work for both simplified (Berggren et al., 1949; Rex, 1950; Colucci, 1985; Nakamura et al., 1997; Hu et al., 2008), and comprehensive models (TN01; Yamazaki and Itoh, 2013; Nakamura and Huang, 2018; Dong et al., 2019).

In Figure 2 near 75-85° W, a characteristic overturning of the Z500 contours indicative of anticyclonic Rossby wave breaking (Masato et al., 2012; Davini et al., 2012) is also observed. Concentrated, large magnitude $\vec{\boldsymbol{W}}$ are found just upstream of, and propagating into the block, and a relative absence of large magnitude $\vec{\boldsymbol{W}}$ occur downstream of the block. On the upstream, equatorward flank of the block, converging $\vec{\boldsymbol{W}}$ consistent with a slowing of the zonal mean flow is observed.~~ (Fig. 2).~~ The behavior of $\vec{\boldsymbol{W}}$ during the genesis of this block case study agrees with Nakamura et al. (1997) and TN01 and is consistent with Nakamura and Huang's (2018) description of blocking as a traffic jam of wave activity fluxes~~(1997) and TN01~~.

Block~~We use block~~-centered compositing analysis is used to confirm that, on average, the blocks identified in the aquaplanet model evolve in a dynamically similar manner to models with zonally asymmetric forcing.~~results shown in previous studies.~~ Figure 3 shows block centered composites of Z500'~~, and~~ $\vec{\boldsymbol{W}}$, and $\nabla \cdot \vec{\boldsymbol{W}}$ for ~~the aquaplanet~~ blocks in the SH midlatitudes (i.e., occurring between 30° and 65° of latitude) of ERA-Interim (ERAI SH, left column, Figs. 3a-c), the aquaplanet midlatitudes (middle column, Figs. 3d-f), and the East region (see table 1 and figure 1) of the 3 km single mountain configuration (3 km SingleMtn East, right column, Figs. 3g-i). ERAI SH was chosen to avoid the regional variation found in

~~12~~

NH blocking (Nakamura et al., 1997; Davini et al. 2012), however, we remind the reader that surface forcing in the SH is asymmetric (e.g. Berrisford et al.~~).~~ 2007). 3 km SingleMtn East blocks were chosen to subset blocks into those that form near the high-pressure anomaly of stationary waves. Only the 3 km SingleMtn East results are shown because block-centered composites for the different topographic configurations (i.e. 1 km, 2 km, 3 km, and TwoMtn), and "Other" regions yielded similar results (not shown).

The onset of blocking (Fig. 3 top row) in the aquaplanet composite (Fig. 3d) is qualitatively~~is~~ similar to that found in the case study (Fig. 2), ERAI SH (Fig. 3a), and SingleMtn 3k East (Fig. 3g). Minor differences are observed however, such as stronger upstream Z500' gradients in ERAI SH and SingleMtn 3k East, and weaker $\vec{W}$ convergence in SingleMtn 3k East.~~2): a Rossby wave train with low-pressure centers upstream and downstream of the composite block centroid, and a large concentration of~~ ~~$\vec{W}$~~ ~~upstream and entering the block (Fig. 3a).~~ For composites over blocks at maximum strength (Fig. 3 middle row), a similar~~, the wave~~ pattern of $\nabla \cdot \vec{W}$ is observed between the 3 models (Figs. 3b, 3e, and 3h). Convergence of $\vec{W}$ on the downstream, ~~is no longer pronounced and low pressure is concentrated~~ equatorward flank of the composite blocks are enhanced compared to onset, and the envelope of greatest $\vec{W}$ is now within the high-pressure center. Upstream, ~~and~~ downstream, and equatorward low-pressure centers are also evident when the composite blocks are at peak strength, though the pattern is not as clean in idealized model composites (Figs. 3e and 3h) compared to ERAI SH (Fig. ~~of the block (Fig. 3b). Large magnitude~~ ~~$\vec{W}$~~ ~~are concentrated inside the block during this time (Fig.~~ 3b). Also, the equatorward cyclone in ERAI SH (Fig 3b) is further upstream than in the idealized cases.

On the final day (bottom row, Figs 3c, 3f, and 3i), each respective~~, the~~ composite block's Z500 anomaly weakens, and low-pressure is concentrated downstream from the block.~~ (Fig. 3c).~~ Weak values of $\vec{W}$ exit the block downstream of the high-pressure maximum during this time (Fig. 3c, 3f, 3i). This is all consistent with downstream development (Danielson et al., 2005). A net divergence of $\vec{W}$ from the blocked region is indicative of a return to westerly zonal flow as the block dies out.~~3c). The composites shown here for the aquaplanet are qualitatively similar to composites for the model configurations with topography, in terms of the evolution of the Z500' field and~~ ~~$\vec{W}$~~~~.~~

~~These compositing results for the midlatitude blocks in the aquaplanet are similar to previous results from reanalysis (Nakamura et al., 1997; TN01; Nakamura and Huang, 2008) in that: (1) An envelope of maximum~~ ~~$\vec{W}$~~ ~~moves from upstream, to inside the block when it is at its maximum strength, to downstream of the block as the block decays (i.e., Fig. 3a-c), and, (2)~~ The ~~geopotential height field shows the evolution of a wave train that eventually dissipates as~~ ~~$\vec{W}$~~ ~~are passed downstream (Fig. 3a-c). On the other hand, the high-latitude blocks from the aquaplanet display quite different behavior.~~

~~3.2 High-latitude blocking~~

~~13~~

~~As discussed in the methods section, the aquaplanet configuration has a larger amount of high-latitude blocking than the other configurations (Fig. 4a, Table 2). These blocks have multiple unique characteristics, as compared to blocks from all model configurations (including the midlatitude blocks for aquaplanet). Berrisford et al. (2007) report that high-latitude blocking events in the Southern Hemisphere have unique behavior compared to their midlatitude counterparts, e.g., not blocking westerly flow or transient eddies. With this as motivation, we present a separate block-centered analysis of the high-latitude blocks from the aquaplanet integration.~~

~~Figure 4b shows the block centered composite of high latitude aquaplanet blocks during their strongest timestep. High-latitude blocks primarily occur poleward of the primary latitudes of wave activity and synoptic systems. Compared to the midlatitude blocks, the high-latitude blocks do not contain much of any large magnitude~~ ~~$\vec{\boldsymbol{W}}$~~ ~~during their strongest timestep (Figs. 3b and 4b). Nakamura et al. (1997) and TN01 cite~~ ~~$\vec{\boldsymbol{W}}$~~ ~~as an important ingredient in block maintenance, but perhaps this is not so true for high-latitude blocking episodes. Furthermore, the composite of high-latitude blocks has much lower geopotential height anomalies than the midlatitude block composite. This unique behavior of high-latitude blocks in the aquaplanet is consistent with that reported in Berrisford et al. (2007) for high-latitude blocks in the SH.~~

~~High-latitude blocking was also identified in the model configurations with topography, but with lesser frequency (Fig. 4a). Composites comparing high-latitude to midlatitude blocks for each configuration yielded similar results to the aquaplanet (not shown).~~

~~Overall, case studies and~~ block-centered composites for the aquaplanet are qualitatively similar to composites for ERAI SH, and~~show that blocks in~~ the idealized model configurations with mountains in terms of the evolution of Z500', $\vec{\boldsymbol{W}}$, $\nabla \cdot \vec{\boldsymbol{W}}$. The likeness of the aquaplanet to ERAI SH is interesting due to the idealized conditions in the model, as well as the lack of topography. These results show the potential utility of an aquaplanet model for understanding the fundamental physics of blocking. The similarities~~share similar characteristics and dynamics as blocks observed in reality. This holds even when blocks are sorted~~ between blocks in the aquaplanet and the topographic configurations show that blocks behave in a similar manner with or without mountains as a source of zonally asymmetric forcing. Having shown that individual blocking events behave as expected~~midlatitude and high-latitude events. Confident with the representation of blocking~~ in the idealized model, ~~next~~ we now shift our focus to~~on~~ the climatological ~~response of blocking to topography.~~

~~3.3 The effects of topography on winter blocking~~

~~This section focuses on the effect of topography on climatological~~ flow features and blocking climatology~~climatologies. As motivation, we first present results from reanalysis that agree with previously published studies. Then, we investigate the response of the same climatological features in the idealized model to changes in topography~~.

3.~~2~~ Climatological Analysis

The majority of theories on blocking formation and maintenance (summarized in the review by Woollings et al. 2018) imply that stationary waves, storm tracks, and upper level mean flow all might play important roles setting the spatial distribution of blocking frequency. These quantities are now examined for the aquaplanet, reanalysis, and model integrations with mountains. In our discussion of the climatological features in reanalysis and the SingleMtn configurations, we have chosen the following approach: we first discuss the stationary wave because it is the most fundamental metric that changes when adding mountains; then, we discuss blocking and its relationship to the jet stream. We close the analysis with a discussion of the storm tracks. This choice of the order is motivated by recent theory from Nakamura and Huang (2018) that put greater emphasis on the influence of the jet stream and stationary waves on blocking.

3.2.1 The aquaplanet

For the aquaplanet, the stationary wave, storm track, and $\overline{U250}$ are zonally symmetric (Figs. 4a and 4b). However, the blocking climatology is not zonally symmetric after 30 years (Fig. 4b). We find that it takes 250 years for the aquaplanet blocking climatology to approach zonal symmetry (Figs. 4c and 4d). However, for the models with orography, the time to reach convergence is likely not as large. We deduced this from the following analysis: we generate 20-year climatologies using randomly sampled years from our 30-year integrations and compare them. For the for the configurations with orography, the blocking climatology is spatially consistent, whereas, for the aquaplanet, each climatology has a unique spatial distribution (not shown). Therefore, we believe that 30-years of model runs provides a usable level of convergence of the spatial climatology of blocking in the integrations with mountains.

3.2.2 Reanalysis

The different orographic~~topographic~~ configurations of the northern and southern hemispheres produce distinct spatial distributions of general circulation features and atmospheric blocking (Fig.~~. Figure~~ 5).~~ shows the stationary wave, U250 climatology, storm track and blocking climatology for winter in ERA-Interim.~~ Stationary wave patterns can emerge due to land-sea heating contrasts, drag, and flow deflection by topography (e.g. Held et al., 2002).~~orographic geometry.~~ The two strongest regions of anomalous high-pressure in the ~~Northern Hemisphere (~~NH~~)~~ are located on the windward side of the Rocky Mountains, and near the western edge of Europe (Fig. 5a). In the SH, the high-pressure maximum is southwest of South America, and a secondary maximum can be found southeast of Australia (Fig 5b). These results are consistent with previous work (Valdes and Hoskins, 1991; Quintanar and Mechoso, 1995; Held et al., 2002;~~The high near the Rockies is part of a wave train induced by the mountains (e.g.,~~ White et al., 2017).~~The high near Europe is more likely driven by land-sea contrast. The Asian orography also produces a stationary wave response and is an important ingredient for the Pacific jet and storm track (Brayshaw et al., 2009). These results agree with previous studies (Valdes and Hoskins, 1991; Held, 2002; White et al., 2017).~~

Near the high-pressure stationary wave maxima (Figs. 5a-b), regions of suppressed $\overline{U250}$ are apparent (Figs. 5c-d). These regions have been shown to be regions of local maxima for Rossby wave breaking (Abatzoglou and Magnusdottir, 2006;

~~15~~

Bowley et al. 2018). These regions are also where blocks are found to occur most often (Figs. 5c-d), in agreement with previous work (Wallace et al., 1988; Barriopedro et al., 2006; Dunn-Sigouin, 2013; Brunner and Steiner, 2017). According to Nakamura and Huang (2018), strong positive stationary wave anomalies, and weak mean westerlies are conducive to blocking. These conditions act to slow down the "speed limit" on $\vec{\boldsymbol{W}}$, leading to "traffic jams" manifested as blocking episodes. Conversely, regions of strong westerlies, and negative stationary wave anomalies have an opposite effect, hence the suppression of blocking in regions of maximal $\overline{U250}$ (Figs. 5c-d) near climatological lows (Figs. 5a-b).

Focusing next on storm tracks, we see that the entrance of the storm tracks occurs on the northeast edge of the $\overline{U250}$ maxima (Fig. 5a, 5c). The details for this relationship are discussed in Chang et al. (2002) and explored in detail for the N. Atlantic in Brayshaw et al. (2009). In the SH, there are also two local maxima in the storm tracks, and they occur to the southeast of the respective $\overline{U250}$ maxima. At the storm track exit region, transient eddies play an important role in the onset (Colucci 1985) and maintenance of blocks (Shutts, 1983; Nakamura et al. 1997; Yamazaki and Itoh 2013; Pfahl et al. 2015; Wang and Kuang, 2019). This region is also where the stationary wave and blocking maxima occur (Fig. 5). There is one exception in the SH however: the SH storm track exit at the eastern terminus of the Indian Ocean (i.e., 90˚ E) does not coincide with a maxima in blocking or the stationary wave – but it is a region of locally weak $\overline{U250}$.

For the NH (SH) in this dataset, 485 (336) blocking events are found yielding a hemispherically-averaged blocking frequency of 2.7 % (1.6 %). The greater amount of blocking in the NH is typically assumed to be a result of the relative abundance of topographic features. Therefore, we will use configurations of the model to explore the effects of mountains on the spatial distribution and hemispherically averaged statistics of blocking frequency.

3.2.3 Orographic Configurations: Single Mountain of varying height

Here, a~~U250 in the NH has two distinct maxima situated over the eastern coastlines of North America and Asia (Fig. 5a.). These maxima are downstream of the topography. These regions of maximal U250 play a key role in guiding storms and creating storm tracks. The storm tracks are regions where transient eddies are most prevalent in the extratropics (e.g., Trenberth, 1991; Chang et al., 2002). The Northern Hemisphere storm tracks maximize just upstream of the U250 maxima (Figs. 5a and 5c). At the end of storm tracks, Rossby waves tend to break more frequently (Abatzoglou and Magnusdottir, 2006) which is often associated with blocking (Pelly and Hoskins, 2003; Masato et al., 2012).~~

~~The Northern Hemisphere blocking climatology agrees with previous work (Wallace et al., 1988; Barriopedro et al., 2006; Dunn-Sigouin, 2013). In the Pacific basin of the Northern Hemisphere, the spatial maximum in climatological block frequency (blocking maximum) is nearly co-located with the high-pressure anomaly of the stationary wave induced by the Rocky Mountains (Fig. 5a and Fig. 5c). This region is also spatially overlapping with the Pacific storm track exit. For the NH Atlantic basin, the location of the blocking maximum and high-pressure stationary maximum are within close proximity, but both the storm track exit *and* maximum spatially overlap with them (Fig. 5a and Fig. 5c). In the NH, blocks rarely occur near the low-pressure anomalies of the stationary wave (Fig. 5a and Fig. 5c).~~

~~In the Southern Hemisphere (SH), the high-pressure maximum is more poleward than the Northern Hemisphere maxima and stretches from the southwestern tip of South America into a secondary maximum southeast of Australia (Fig 5b). This matches what is reported in Quintanar and Mechoso (1995). Stationary wave features are far less apparent in the Southern Hemisphere, presumably because of the relative lack of topographic forcing compared to the Northern Hemisphere.~~

~~The lack of topographic forcing in the SH allows there to be one distinct band of maximum U250 (Fig 5b). The U250 maximum in the SH stretches from the Indian Ocean into the Pacific and maximizes East of Australia (Fig 5b). The~~ single mountain~~storm track maximizes in the Indian Ocean near Antarctica and stretches from the Atlantic to the Pacific (Fig 5d), far upstream from the region of maximum U250 (Fig 5b and Fig 5d). The SH storm track~~ is added~~as reported in Nakamura and Shimpo (2004).~~

~~In the Southern Hemisphere, our blocking climatology is similar to that reported in Brunner and Steiner (2017). The blocking maximum is near the high-pressure anomaly of the stationary wave and the exit region of the Pacific storm track of the Southern Ocean (Fig. 5b and Fig. 5d). The spatial frequency of blocking in the SH extends into the SH Atlantic storm track entrance region, away from the high-pressure anomaly, but the local blocking maxima in the SH Atlantic is weak compared to the SH Pacific maxima (Fig. 5d).~~

~~Topographic differences yield contrasting spatial distributions of stationary waves, U250, storm tracks, and blocking between the hemispheres. These observations lead~~ to the aquaplanet~~specific questions this subsection seeks~~ to study the response of the idealized model ~~address:~~

~~- What effect does topography have on~~ blocking climatology to the presence of orography. Figure 6 shows the~~?~~
~~- What role do~~ stationary -waves ~~and storm track exit regions have in setting the locations and intensity of blocking maxima?~~

~~**3.3.2 Blocking in idealized model experiments**~~

~~The idealized model configurations allow us to systematically investigate the response of atmospheric circulation and blocking to topography. As we did for reanalysis, for each model configuration we examine the stationary wave, U250~~, storm tracks, ~~and the~~ blocking climatologies, and $\overline{U250}$~~climatology.~~

~~***Stationary wave***~~

~~As expected, a stationary wave is absent~~ in the SingleMtn integrations. In each integration,~~aquaplanet (Fig. 6a), and upon introducing topography, zonally asymmetric forcing is imposed, and~~ a stationary wave is induced (Figs. 6a~~6b~~-6d) with~~).~~ ~~SingleMtn contains~~ a high-pressure anomaly generated near the coastline on the windward side of the mountain, and a low-pressure anomaly on the leeward side (Fig. 6a-d~~6b~~). This results in a meridionally tilted stationary wave pattern that extends into the subtropics leeward of the mountain. This pattern has been explained in previous idealized modeling work (Grose and Hoskins, 1979; Cook and Held, 1992; Lutsko 2016). The intensity and zonal extent~~high-pressure anomaly extends~~

~~17~~

~~approximately 180° of longitude upstream~~ of the stationary wave extrema increases with mountain height (Figs. 6a-d). ~~and weakens from east to west.~~

In ~~SymMtn,~~ the ~~configuration with two mountains and equal-sized ocean basins, each mountain induces a meridionally tilted stationary wave pattern (Fig. 6c) similar to that in~~ SingleMtn integrations, as the height of the mountain is increased~~(Fig. 6b). The zonal extent of the high- and low-pressure anomalies in the SymMtn stationary waves, however, are suppressed compared to SingleMtn. This suppression is due to interference of stationary waves induced by multiple sources of topographic forcing (Manabe and Terpstra, 1974; Held et al., 2002; White et al., 2017).~~

~~For AsymMtn~~, the ~~placement of the topography creates two ocean basins of different zonal extents: a short basin and a wide basin. Like SymMtn, each mountain in AsymMtn induces a meridionally tilted stationary wave, however, the asymmetric configuration of the mountains results in asymmetric zonal extent in the anomalies (Fig. 6d). In the short basin, the anomalies have less zonal extent than those in SymMtn, and the opposite holds true for the wider basin. Further comparing the two basins, we find the high-pressure anomaly in the wide basin extends 100 degrees westward from the mountain, much farther than that of the short basin. This extended high-pressure anomaly is related to blocking, which we will further address below, but first we analyze U250.~~

~~***250 hPa zonal wind climatology***~~

~~In the aquaplanet, U250 is zonally symmetric. When topography is added, localized regions of U250 maxima occur. In SingleMtn, the U250 maximum occurs on the leeward side of the mountain, equatorward of the low-pressure anomaly (Fig. 6b). The stationary wave pattern associated with the topography generates cold advection towards the southeast on the lee of the mountain. This is due to both the change in wind direction created by the mountain and the differences in heat capacity for the topography as compared to the ocean. The cold advection leads to a~~ local maximum in the $\overline{U250}$ increases as well (right column, Fig 6). This relationship between the strength of the local jet maxima and mountain height follows from the thermal wind relationship and the increased~~meridional~~ temperature gradient in the lower troposphere downstream of the mountain. This mechanism is also apparent in Brayshaw et al. (2009). The stronger ~~east of the topographical feature (not shown). Related to this~~ temperature gradient is~~, the U250 maximum must exist~~ due to enhanced cold advection in the runs with taller mountains.~~thermal wind balance.~~ This pattern of the $\overline{U250}$~~U250~~ maximum occurring just downstream of mountains is the same as what occurs for the NH in observations (Fig. 5a). Across models, localized strengthening near

~~In SingleMtn there is also a relative suppression of U250 nearly 120° downstream of~~ the ~~mountain, from about 150° W – 110° W, followed by a secondary~~ maximum $\overline{U250}$ is accompanied by a weakening of $\overline{U250}$~~of U250 from roughly 110° W - 0°. The disjointed distribution of U250 is perhaps a consequence of blocking and will be discussed~~ further ~~in the blocking climatology subsection.~~

~~The U250 maxima for SymMtn and AsymMtn are located on the poleward side of the low-pressure anomalies of each configuration's stationary waves (Figs. 6c-6d). This is due to the same cold advection-generated temperature gradient~~

~~explained for SingleMtn. In AsymMtn Short Basin however, the zonal extent of the U250 maximum produced by the upstream mountain is suppressed – likely because of influence from the~~ downstream. In regions poleward ~~mountain, and consistent with the zonal suppression of the stationary wave (Fig. 6d).~~

~~The U250 field acts as a waveguide for synoptic scale Rossby Waves (e.g. Wirth et al. (2018). The waveguide coincides with preferred regions where transient Rossby Waves are generated and propagate. These regions are also known as storm tracks (e.g. Chang et al., 2002), which is the next topic of our discussion.~~

~~***Eulerian storm track***~~

~~The storm track in the aquaplanet is zonally symmetric (Fig. 6e), while the topographical configurations have zonally asymmetric storm tracks whose locations are set by mountains (Figs 6f-6h). In the topographic configurations, the storm tracks almost exactly overlap with the U250 maxima, with the exception that the storm track maxima are slightly upstream from the U250 maxima (Figs 6b-6d, Figs 6f-6h). In AsymMtn Short Basin, the zonal extent of the storm track is suppressed by the topographical spacing, similar to U250 and the stationary wave.~~

~~Previous studies have shown that the storm track exit region coincides with the terminus~~ of the midlatitude ~~wave guide (e.g. Wirth et al., 2018), and the exit region is the primary region where Rossby wave breaking occurs (Strong and Magnusdottir, 2008; Davini et al., 2012). The storm track exit region can interact with the stationary wave, and as discussed in the next section, the storm track exit proves to be very important in where and how frequently blocks occur.~~

~~Blocking climatology~~minimum in $\overline{U250}$, blocking is most abundant (Figs. 6e-h). This region also coincides with the high-pressure maximum of the stationary wave (Figs. 6a-d). The weakened flow and positive stationary wave anomaly here are consistent with a region of lowered $\vec{\boldsymbol{W}}$ "speed limit" (Nakamura and Huang, 2018), and thus enhanced block frequency. Figures 6e-h shows that these regions have

~~The blocking climatology in the aquaplanet is not zonally symmetric for the 30-year integration (years 11-40; Fig. 6e). For a 300-year integration, the climatology is much closer to being zonally symmetric, though it has still not converged (not shown). No zonal asymmetries in forcing exist in the aquaplanet, so the zonal asymmetries attest to the internal variability and relative rarity of blocking events identified in the aquaplanet. The configurations with topography are closer to reaching convergence after 30 years – in terms of the local maxima occurring just west of the topography. To demonstrate this, we compare climatologies of Aquaplanet and AsymMtn based on randomly chosen subsets of years. Aquaplanet blocking climatologies using randomly sampled years produce results with varying spatial frequencies (Fig. 7).~~

~~Upon adding topography, spatial maxima form in the blocking climatology (Figs. 6e-6h) and~~ significantly more blocking compared to the extended aquaplanet run. On the other side of the mountain, block frequency is significantly suppressed near the low-pressure stationary wave anomaly, poleward of the $\overline{U250}$ maximum.~~occurs overall (see Table 2 for quantitative differences). The result that adding topography to our model leads to greater block frequency matches with observations, since~~

~~the Northern Hemisphere contains a relative abundance of topography and blocking, when compared to the Southern Hemisphere (Figs. 5c-5d).~~

The presence of mountains also leads to localized storm track maximum in each of the SingleMtn configurations (Figs. 6a-d). The storm track maximum straddles the stationary wave minimum immediately downstream of the region where the $\overline{U250}$ maximum also occurs (Fig. 6e-h). The storm track exit region in the idealized model does not coincide with the high-pressure stationary anomaly, as it does in the NH of Earth. This allows one to work toward decoupling the response of blocking to each feature. The main blocking maximum occurs near the stationary wave maximum, which is 60˚ longitude east of the storm track exits. Near the storm track exit region, where the stationary waves are near neutral (i.e. near 90 W), there are suggestions of secondary blocking maxima (Fig. 6e-h). This region is perhaps related to the breaking of Rossby waves at the end of the storm track and a local block genesis region associated with strong extratropical cyclones. This would be consistent with theories linking blocking to Rossby wave-breaking (Pelly and Hoskins, 2003; Berrisford et al., 2007; Masato et al. 2012).

The zonal extent of the blocking climatology maximum increases when mountain height is increased (Figs. 6e-h). This agrees with the response of the stationary wave (Figs. 6a-d). The overall hemispherically averaged statistics of blocking frequency yields an increase in blocking when mountain height is increased (See Table 2). These increases for the 2k-4k configurations are modest however and should be taken with some degree of caution. Still, it is clear that as mountain height increases, there is a greater area of significantly more blocking compared to the aquaplanet (Figs. 6e-h). Next, we investigate the response of adding an additional mountain.

3.2.4 Topographic Configurations: 2 Mountains

For this analysis, two 3 km-high Gaussian mountains centered at 45° N with 120° of longitude between them are added to the aquaplanet. The placement of the mountains is meant to create a wide and short ocean basin, as observed in the NH of earth. 3 km height is meant to be semi-realistic; the values are lower than the maxima for the Rockies and the Himalayas – however the mountains are substantial enough to have generate obvious changes in the circulation (as evidenced in the Single Mountain experiments).

The addition of a second mountain induces a second trough and ridge in the stationary wave, and a second maxima for the blocking climatology, storm track, and $\overline{U250}$ (Fig. 7). The intensity and zonal extent of these features, however, varies with respect to each mountain and is a result of interference between the forcing (Manabe and Terpstra, 1974; Held et al., 2002; White et al., 2017).

The TwoMtn configuration has a greater hemispherically averaged blocking frequency than the other configurations (Table 2). This is despite the TwoMtn configuration having a lower total number of blocks than the 3 and 4 km SingleMtn configurations, respectively – meaning the blocks have a longer average duration in the 2-~~The blocking maximum in SingleMtn (Fig. 6f) is slightly upstream from the maximum high-pressure anomaly (Fig. 6b), on the windward side of the~~

~~20~~

~~topography. This is similar to the NH Pacific blocking maximum being situated northwest of the Rocky Mountains in observations (Fig. 5c). The high-pressure anomaly on the windward sides of mountains acts as a source region of anticyclonic vorticity and can be recognized as ridges in instantaneous maps of geopotential height. These ridges serve as precursors for topographically induced blocks, which are then amplified and maintained by transient eddies and~~ $\cancel{\vec{W}}$ ~~(Nakamura et al., 1997; TN01).~~

~~A secondary blocking maximum in SingleMtn is found towards the western end of the high-pressure anomaly, near the storm track exit (Fig. 6f). A tertiary, but relatively weak blocking maximum is found from roughly 150° W – 110° W, where U250 contains a local minimum in between the two U250 maxima. The blocking in this region is a probable explanation for the gap in the U250 maximum, as blocks are known to inhibit or even halt zonal flow. The second and third blocking maxima are consistent with current theory linking blocking to Rossby wave-breaking (Pelly and Hoskins, 2003; Berrisford et al., 2007; Masato et al. 2012), which as mentioned before, predominantly occurs at the storm track exit. Each of the 3 blocking maxima in SingleMtn are found to be unique regions of block genesis.~~

~~The presence of a second, symmetrically placed mountain in SymMtn leads to the occurrence of significantly more blocking than in the aquaplanet, SingleMtn, and even AsymMtn (Fig. 6g and Table 2). The blocking maxima in SymMtn sit near the intersection of the high-pressure anomaly and storm track exit (Fig 6c and Fig. 6g). In AsymMtn there are blocking maxima also on the windward sides of the mountains near each respective high-pressure anomaly (Fig. 6h), and the overall area-averaged block frequency is slightly greater than SingleMtn, but less than SymMtn (Table 2).~~

~~In AsymMtn Wide Basin, the blocking maximum is close to the stationary wave maximum and a secondary blocking maximum occurs at the western edge of the high-pressure anomaly, near the storm track exit (Fig. 6d and 6h). As in SingleMtn, these separate maxima correspond to distinct block genesis regions.~~

~~In AsymMtn, the short basin has a greater block frequency maximum than wide basin (Fig. 6h). Like SymMtn, the short basin in AsymMtn has a storm track exit region that overlaps with the high-pressure maximum of the stationary wave when compared to SingleMtn and AsymMtn Wide Basin. This perhaps explains the enhanced blocking climatological maximum in AsymMtn Short Basin compared to AsymMtn Wide Basin. On the other hand, AsymMtn Short Basin has such a small zonal extent that the storm track exit overlaps with the~~ mountain configuration (Table 3). Each mountain also creates regions of enhanced and suppressed blocking frequency (Fig. 7b). However, just like the general circulation features,~~. Thus, in this short basin~~ there are differences in the blocking climatology for the two ocean basins.

Next, we examine the blocking climatology within each of the two ocean basins in the TwoMtn simulation (Wide Basin and Short Basin, respectively, see Fig. 1 and Table 1). In the Wide Basin, there is close to a basinwide enhancement of blocking frequency when compared to the single mountain cases (Figs. 6e-h, and 7b). Consistent with this enhancement, the overall midlatitude $\overline{U250}$ climatology is much weaker in the wide basin compared to the other ocean basin and SingleMtn integrations. In the Short Basin, a separate blocking maximum exists near the high-pressure stationary wave anomaly. This maximum, albeit much weaker than its wide basin counterpart, is still significantly more than what occurs in the same region for the aquaplanet.

The proximity of the storm track maximum in the short basin makes there more likely to be times in which storm development occurs just upstream of the mountain; this coupled with a strong background westerly flow would inhibit blocking and perhaps explains the discrepancies between the wide basin and short basin maxima. The shorter ocean basin containing much less blocking is not consistent with what is observed in the NH of Earth, where the Atlantic has a slightly stronger blocking maximum. It seems more elaborate landmasses than this simplified case are needed to better simulate what is observed between the Atlantic and Pacific blocking climatologies in the NH.~~ and such conditions would inhibit blocking.~~

3.3 Block Duration Statistics

~~As observed in the Atlantic basin of Earth, we suspect the shortened jet in AsymMtn Short Basin acts as a waveguide that funnels transient eddies and $\vec{W}$ into the anticyclonic anomaly of the stationary wave, and these eddies have the potential to feed blocks or help destroy them. The details of those processes are a focus of future work.~~

~~When comparing the blocking climatologies for each configuration, we find that blocks are predominantly generated at high-pressure stationary maxima, regions dominated by wave breaking (storm track exit), or at some spatial mixture of the two (Figs. 6e-6h). The aquaplanet shows that blocks can arise purely from eddy-eddy interactions, whereas the other configurations show that blocks can also be induced by topography, at a more frequent rate.~~

~~We want to highlight the result that SymMtn has the largest area-averaged block frequency (Table 2) and number of events (Table 3) out of all the configurations. We hypothesize that this is because the ocean basins in SymMtn have a zonal extent that allows a synergy between the block genesis mechanisms associated with the high-pressure anomaly induced by the topography and block maintenance mechanisms associated with the storm track exit. A similar inference can be made when comparing the short and wide basins of AsymMtn, where the short basin contains a stronger blocking maximum and a more spatially coincident storm track exit with the high-pressure of the stationary wave. However, as mentioned above, AsymMtn Short Basin is so short that there is not enough spatial separation between the storm track entrance and the downstream topographical feature. The processes governing the interactions of the storm tracks and the topographical features in relation to blocking are topics of future work.~~

~~3.4 Block duration and displacement~~

One of the characteristics that allows blocks to influence midlatitude weather is their persistence. As such, we examine the influence of mountains~~topography~~ on block persistence using our duration metric. First, we find that adding mountains leads to at least a modest increase in the average midlatitude block duration (Table 3). All topographic configurations aside from 1 km SingleMtn, also have 7-39 more blocks than the aquaplanet (Table 3). This helps to explain some of the climatological differences in block frequency between the idealized model configurations (Table 2), particularly for the 1 km SingleMtn case.

Despite a 0.25 day greater mean block duration (Table 3), 1 km was found to have less hemispherically averaged blocking than the aquaplanet (Table 2) due to 21 less events. The blocks in the topographic integrations were then put into subsets based off those originating near the high-pressure stationary wave anomaly and those that were not~~First, we find that adding topography, regardless of configuration, leads to longer duration blocks on average (Table 3). For SingleMtn, the difference compared to Aquaplanet is statistically significant (8.4 versus 7.3 days, respectively). For SymMtn and AsymMtn, the mean duration is longer, but the difference is not significant at the 85th percentile. This is because of the large variance in block duration when we consider all midlatitude blocks generated by the model. However, if we subset the blocks, based on the location in which they are generated, this result changes~~.

Regions used to subset blocks are denoted as “East”, those originating at the eastern end of the ocean basin near the high-pressure stationary anomaly, and “Other”, those originating elsewhere in the midlatitudes (Fig. 1a and Table 1). Figure 8 shows the probability density functions for the aquaplanet and SingleMtn East blocks. With the exception of the 4 km run, the “East” regions of the single mountain integrations have relatively less shorter duration blocks (i.e. 5-11 days), and relatively more longer duration blocks (11 days or more) compared to the aquaplanet (Fig. 8). Blocks from the “East” regions last longer on average than aquaplanet blocks (Table 3), but the 3 km and 4 km enhancement of block duration are not significant to the 95th percentile. Mean block duration is greater for the “East” region compared to the “Other” in the single mountain configurations (Table 3), with significant differences found in the 1 km and 2 km integrations. This leads to a cautious suggestion that blocks that originate near mountains last longer on average than those that do not, though the modest differences found in the 3 km and 4 km integrations must be considered.

The response of the TwoMtn configuration is much less straightforward. This integration is divided into 3 regions, Wide Basin East, Wide Basin Other, and Short Basin (Fig. 1b and Table 1); Note the Short Basin does not have distinct “East” and “Other” regions because of its shortened zonal extent. Average block duration in the “Other” region in the Wide Basin is slightly longer than the “East”, but both regions are significantly greater than the Short Basin. This coupled with more Wide Basin East events (Table 3) is consistent with the weaker maximum in the blocking climatology for the Short Basin (Figure 7b). Perhaps this is related to the inhibition of blocking by the nearby storm track and $\overline{U250}$ maximum in the Short Basin, but we do not seek to attribute a causal relationship here.

Our results suggest that blocks starting near mountains last longer on average than those that do not (Table 3). In reality we see a similar situation where the NH has more orographic forcing compared to the SH, and also a longer average block duration (8.0 days for the NH and 6.9 days for the SH). In the idealized model, the compositing analysis for the aquaplanet shows similar forcing patterns by low frequency eddies ($\nabla \cdot \vec{\boldsymbol{W}}$) when compared to the SingleMtn East blocks (Figs. 3d-i), despite having a shorter average block duration. Perhaps these duration differences can be accounted for by considering block maintenance by high frequency transients (Shutts, 1983; Nakamura et al., 1997; TN01; Yamazaki and Itoh, 2013; Wang and Kuang, 2019). High frequency eddy forcing has yet to be investigated in these experiments, but this will be a topic of future work.

4. Discussion

To add some perspective on the role of mountains as compared to land masses with no orographic features, we analyze the response of an idealized model configuration with a single flat land mass, herein referred to as 0 km (Fig. 9). The results of 0 km are briefly mentioned here to primarily serve as a benchmark for this setup. This configuration is like the others that include mountains in that it imposes zonally asymmetric forcing in land-sea contrast and orographic drag (Pithan et al., 2016); The difference, however, is that that the flat land does not act a direct barrier that deflects the flow as the mountains do, generating a unique stationary wave response (e.g. Held et al. 2002) (Figs 6a-d, 7a, and 9).

The response of $\overline{U250}$ and the storm track (Fig. 9) in 0 km agree with results by Brayshaw et al. (2009). Compared to the single mountain runs, the stationary wave pattern is shifted upstream in 0 km (Figs. 6 and 9). The blocking climatology maximizes (minimizes) poleward of regions where the midlatitude $\overline{U250}$ minimizes (maximizes) (Fig. 9b). In the single mountain integrations, the maximum in the blocking climatology is nearly co-located with the maximum in the stationary wave; For the 0 km integration, it is not. The high-pressure stationary anomaly seemingly plays less of a role in the flat case. The 0 km integration has a 3.42 % hemispherically averaged block frequency, which is greater than the aquaplanet and 1 km configurations but less than the others with taller mountains (Table 2).

5~~Using the regions defined in Table 1, we found that for blocks that occur in the eastern portion of the ocean basins (i.e., East Blocks), the mean durations are all significantly longer than those of aquaplanet (Table 4, and see Fig. 8.b. for the probability density distributions). The east portion of the ocean basins is near the local maxima in the stationary wave west of the topography, thus, the longest duration blocks per configuration are those that are generated just upstream of topography. Furthermore, the average duration values for the East blocks in SingleMtn and AsymMtn are greater than their Mid counterparts (i.e. blocks that start near the storm track exits, see Table 1 and Fig. 6). SingleMtn East and SingleMtn Mid have mean block durations of 9.1 and 8.2 days respectively (Table 4). AsymMtn Wide Basin East and AsymMtn Wide Basin Mid have significantly different mean block durations of 8.3 and 7.1 days respectively (Table 4). Thus, blocks that form near topography in this model (i.e., the East blocks), tend to persist for longer times than those that form far from topography (i.e., Mid blocks, or blocks in the aquaplanet configuration). The same analysis applied to the NH and SH in reanalysis found that the NH, which presumably contains much more topographically forced blocks, has an average block duration (8.0 days) that is significantly longer than those from the SH (6.9 days).~~

~~A natural question to ask then is: Why do blocks originating near topography have longer durations than those in the aquaplanet? Given that the topographic configurations contain both stronger localized storm track regions and blocks generated by topography, whereas the aquaplanet does not, we hypothesize two possible explanations for the differences in duration:~~

~~24~~

~~1. The stronger localized storm tracks create more eddies, which would provide more transient eddies that could feed the blocks through dry dynamics (e.g., Shutts, 1983; TN01; Yamazaki and Itoh, 2013) or moist dynamics (Pfahl et al., 2015).~~

~~2. Topographically generated blocks last longer than blocks predominantly generated by eddy-eddy interactions because they are fundamentally different.~~

~~Regarding Hypothesis 2, we analyzed $\vec{W}$ composites for East Blocks as compared to Mid Blocks and found minimal differences aside from increased composite $\vec{W}$ magnitudes for the Mid Blocks (Fig. 9). Since the Mid blocks are those more likely to be generated by eddy-eddy interactions, this result refutes Hypothesis 2. Related to this, as discussed in Sect. 3.1, the life cycle composites of the wave activity flux are very similar for the aquaplanet configuration and the configurations with topography (i.e. Fig 3 and Fig. 9). These results point more toward hypothesis 1 but are very much preliminary. More work is planned to investigate the maintenance of blocking between the model integrations.~~

~~Next, we test for differences in block displacement to determine if topography obstructs the movement of blocking events. The differences in average block displacement (Table 3) between the four configurations are small. When comparing East, Mid, and the aquaplanet blocks, the differences are also small. Even when isolating just the AsymMtn Wide Basin East and AsymMtn Short Basin blocks, the difference in average block displacement is still slight. Thus, even with topographic obstructions, block displacement is not affected.~~

4. Summary and conclusions

This work utilizes an idealized moist GCM to better understand atmospheric blocking. We start with an analysis of blocking in an aquaplanet, then~~. Then we~~ systematically add mountains~~topographic features~~ to investigate the influence of orography~~topography~~ on blocking frequency and ~~, in terms of their climatological location,~~ duration~~, and displacement~~.

Using~~In~~ the aquaplanet we confirm~~find~~ that blocks can be generated purely through eddy-eddy interactions, without any zonally asymmetric~~; i.e., they do not require surface~~ forcing from the surface.~~.~~ This result substantiates the results of~~agrees with~~ Hu et al. (2008),~~) and~~ Hassanzadeh et al. (2014), and Nabizadeh et al. (2019).~~which are, to our knowledge, the only other aquaplanet studies related to blocking.~~ To expand on the results of those previous studies, we~~ qualitatively~~ examined the dynamical life cycle of the blocks in the aquaplanet. Block centered composites of Z500' and $\vec{W}$ show that block lifecycles in the aquaplanet include: ~~include large-scale Rossby wave features with $\vec{W}$ entering the block during onset, followed by concentrated $\vec{W}$ inside the block during peak strength, and ending with $\vec{W}$ emitted downstream of the block into low-pressure regions during decay. This behavior is similar to what is found in nature (e.g., TN01).~~

(1) Large-scale Rossby wave features with $\vec{W}$ entering the block and converging on the upstream-equatorward flank during onset

(2) Stronger $\vec{W}$ convergence and greater concentrations of $\vec{W}$ inside the block during peak strength

(3) A net divergence of $\vec{W}$ emitted downstream of the block into low-pressure regions during decay

Similar behaviour is shown for reanalysis and the idealized model configurations that include orography, affirming the usefulness of a simple idealized aquaplanet model in better understanding blocks observed in reality.

In ~~Like Berrisford et al. (2007), who looked at blocking in Earth's Southern Hemisphere, we identify distinct high-latitude blocking events that differ from midlatitude blocks. High-latitude blocks in the aquaplanet have lower geopotential height anomalies, primarily occur poleward of the main zonal channels of~~ $\vec{W}$~~, and do not contain strong concentrations of~~ $\vec{W}$ ~~at peak strength. This suggests an alternative maintenance mechanism for high-latitude blocks than those proposed for blocks in general by Nakamura et al. (1997) and TN01. High-latitude blocks are also identified in the topographic configurations, but to a lesser extent than the aquaplanet.~~

~~For the topography~~ experiments with orographic forcing, we modified the aquaplanet model in the following ways: (1) adding a single ~~3-km~~ mountain of different heights in separate integrations; and, (2) in another integration, ~~; (2)~~ adding two 3-km high mountains placed in a manner that creates one wide~~evenly spaced with respect to longitude; and, (3) adding two 3-km mountains asymmetrically space with respect to longitude, to create one long~~ and one short ocean basin.

The addition of mountains to the idealized model~~topography~~ led to several~~some~~ changes in blocking when~~that were universal across all configurations with topography,~~ compared to the aquaplanet integration:

- There are localized maxima in blocking, upstream of mountains~~topography~~; near the high-pressure maximum of the stationary waves; poleward and near climatological minima in $\overline{U250}$.~~a source region of anticyclonic vorticity.~~
- There are localized minima in blocking, downstream of mountains; near the low-pressure anomaly of the stationary wave; poleward and near climatological maxima in $\overline{U250}$.
- There is a significant increase in hemispherically averaged blocking frequency in integrations with mountains of height 2 km and greater.
- There~~There is significantly more wintertime blocking overall with topography present.~~
- ~~When topography~~ is an increase in block duration for~~present,~~ blocks originating near mountains, though the statistics are~~have longer durations.~~
- ~~Topography does~~ not robust~~play a key role in determining the characteristics of block movement~~.

Based on ERA-Interim reanalysis, these results mirror what is observed for the NH and SH, where the NH contains more topography and blocking. In the idealized model, the enhancement of block frequency near the stationary wave maximum and $\overline{U250}$ minimum is consistent with these regions being conducive to the convergence (or "traffic jamming") of wave activity fluxes. These regions are found to be far from ~~, blocking, and longer lasting blocks.~~

~~The addition of topography also induces stationary waves, and localized maxima in the jet streams and~~ the storm ~~tracks. This response has been documented previously, but our interest was the interaction between these features and blocking.~~

~~In all configurations with topography, local blocking maxima are found near high-pressure stationary anomalies as well as storm~~ track exit however, which is dissimilar to the NH in reanalysis. At the~~regions, where Rossby waves tend to break. A local minimum in blocking is coincident with the jet stream maxima and storm track entrance regions.~~

~~The spacing between the two mountains is important for the amount of blocking that is produced: symmetrically placed mountains leads to significantly more blocking than all other configurations. Both blocking maxima in SymMtn spatially overlap with their ocean basin's respective~~ storm track exit region in the North Atlantic, previous work has shown that extratropical cyclones can seed blocks (Colucci 1985) or maintain them, Pfahl et al. (2015). However, the storm track exit coincides, or sits spatially close to the~~and anticyclonic~~ stationary wave maxima. In our single mountain experiments,~~anomaly. We suspect SymMtn's increased block frequency reflects a spatial resonance between breaking Rossby waves at~~ the storm track exit is far from the stationary wave maxima,~~exits interacting with high-pressure anomalies generated by the mountains. This helps explain some of the differences in the blocking climatology we observe between the Pacific~~ and the result is that the blocks preferentially occur at the stationary wave maxima region. This suggests that the role of the cyclones in nature may be secondary to the role of the large-scale flow. That being said, secondary~~Atlantic in the NH.~~

~~Though the~~ blocking maxima ~~in the NH Atlantic and Pacific basins are similar in magnitude, the Pacific maximum covers a larger area – thus there is more blocking in the Pacific. In the NH Pacific, a similar spatial distribution to SymMtn is observed between the storm track exit, blocking maximum and stationary wave induced by orography. The Atlantic on the other hand, is akin to the Short Basin in AsymMtn, a storm track whose exit and maximum both~~ are found near the storm ~~semi-coincident with the stationary high-pressure and blocking maximum. Our results suggest the broader Pacific blocking maximum is a consequence of better spatial resonance between the Pacific storm~~ track exit ~~and stationary anomaly, compared to the Atlantic. An alternative hypothesis is that the semi-coincidence between the storm track and blocking maxima~~ in the idealized model, suggesting that this~~Atlantic inhibits blocking. Another possible explanation is that the stationary wave in the Atlantic is forced by land/sea contrasts rather than a mountain, leading to different interactions with its storm track, as compared to the Pacific. Further work will be done to investigate the sensitivity of climatological blocking maxima to the~~ location also plays a key role in anchoring where blocks most frequently occur~~of storm track exits~~.

~~In the configurations with topography, blocks generated near topography last longer, on average, than those produced away from topography. However, compositing results of Z500' and $\vec{\boldsymbol{W}}$ found blocks forming near and away from topography yielded little differences aside from blocks away from topography interacting with larger magnitudes of $\vec{\boldsymbol{W}}$ compared to near topography counterparts. Further work is planned to provide a mechanistic explanation for these differences we find in block duration.~~

Overall, this work elucidates fundamental information on the formation, dynamical evolution, spatial distribution, ~~duration, and displacement of atmospheric blocking. Future work will utilize a suite of dynamical diagnostics to take a deeper look into the differences between blocks generated near topography compared to those that are not, and how it relates to what is observed in reality.~~

and duration of atmospheric blocking – both in an aquaplanet and configurations with zonally asymmetric forcing. One limitation in the two-mountain experiment, is that each mountain simultaneously affects the stationary wave, jet, and storm track, making it difficult to tell the order of influence each has on the blocking climatology. Understanding the interplay and individual effects of these flow features is key to predicting the behavior of blocks in future climates. This is a topic of future work.

~~28~~

Acknowledgements:

This study is supported and monitored by The National Oceanic and Atmospheric Administration – Cooperative Science Center for Earth System Sciences and Remote Sensing Technologies under the Cooperative Agreement Grant #: NA16SEC4810008. The authors would like to thank The City College of New York, NOAA Center for Earth System Sciences and Remote Sensing Technologies, and NOAA Office of Education, Educational Partnership Program for fellowship support for Veeshan Narinesingh, and the American Society for Engineering Education for their support of Spencer K. Clark through a National Defense Science and Engineering Graduate Fellowship. The statements contained within the manuscript are not the opinions of the funding agency or the U.S. government, but reflect the authors' opinions.

~~29~~

References

Abatzoglou, J. T., and Magnusdottir, G.: Planetary Wave Breaking and Nonlinear Reflection, J. Climate, 19, 6139-6152, doi:10.1175/JCLI3968.1, 2006.

Barnes, E., Slingo, J., and Woollings, T.: A methodology for the comparison of blocking climatologies across indices, models and climate scenarios. Clim. Dynam., 38, 2467-2481, doi:10.1007/s00382-011-1243-6, 2012.

Barriopedro, D., GarcÍa-Herrera, R., Lupo, A. R., and Hernández, E.: A Climatology of Northern Hemisphere Blocking. J. Climate, 19, 1042-1063, doi:10.1175/JCLI3678.1, 2006.

Barriopedro, D., García-Herrera, R., and Trigo, R.: Application of blocking diagnosis methods to General Circulation Models. Part I: a novel detection scheme. Clim. Dynam., 35, 1373-1391, doi:10.1007/s00382-010-0767-5, 2010.

Berggren, R., Bolin, B., and Rossby, C.-G.: An Aerological Study of Zonal Motion, its Perturbations and Break-down. Tellus, 1, 14-37, doi:10.3402/tellusa.v1i2.8501, 1949.

Berrisford, P., Hoskins, B. J., and Tyrlis, E.: Blocking and Rossby Wave Breaking on the Dynamical Tropopause in the Southern Hemisphere. J. Atmos. Sci., 64, 2881-2898, doi:10.1175/JAS3984.1, 2007.

Booth, J. F., Dunn-Sigouin, E., and Pfahl, S.: The Relationship Between Extratropical Cyclone Steering and Blocking Along the North American East Coast. Geophys Res. Lett., 44, 11-11,984, doi:10.1002/2017GL075941, 2017.

Booth J. F., Kwon, Y.-K., Ko, S., Small, J., Madsek, R.: Spatial Patterns and Intensity of the Surface Storm Tracks in CMIP5 Models. Journal of Climate, 30, 4965–4981. 2017.

Bowley, K. A., Gyakum J. R., and Atallah E. H.: A New Perspective toward Cataloging Northern Hemisphere Rossby Wave Breaking on the Dynamic Tropopause. Mon. Weather Rev., 147, 409-431, doi:10.1175/MWR-D-18-0131.1, 2019

Brayshaw, D. J., Hoskins, B., and Blackburn, M.: The Basic Ingredients of the North Atlantic Storm Track. Part I: Land–Sea Contrast and Orography. J. Atmos. Sci., 66, 2539-2558, doi:10.1175/2009JAS3078.1, 2009.

Brunner, L., Schaller, N., Anstey, J., Sillmann, J., and Steiner, A.: Dependence of Present and Future European Temperature Extremes on the Location of Atmospheric Blocking. Geophys. Res. Lett., 45, 6311-6320, doi:10.1029/2018GL077837, 2018.

Brunner, L., A. Steiner, 2017: A global perspective on atmospheric blocking using GPS radio occultation – one decade of observations. Atmospheric Measurement Techniques, 10, 4727-4745, doi:10.5194/amt-10-4727-2017.

Cassou, C., Terray, L. and Phillips, A. S.: Tropical Atlantic Influence on European Heat Waves. J. Climate, 18, 2805-2811, doi:10.1175/JCLI3506.1, 2005.

Charney, J. G., DeVore, J. G.: Multiple Flow Equilibria in the Atmosphere and Blocking. J. Atmos. Sci., 36, 1205-1216, doi:10.1175/1520-0469(1979)036<1205:MFEITA>2.0.CO;2, 1979.

Clark, S. K., Ming, Y., Held, I. M., and Phillips, P. J.: The Role of the Water Vapor Feedback in the ITCZ Response to Hemispherically Asymmetric Forcings. J. Climate, 31, 3659-3678, doi:10.1175/JCLI-D-17-0723.1, 2018.

~~30~~

Clark, S. K., Ming, Y., and Adames, Á. F.: Monsoon low pressure system like variability in an idealized moist model. J. Climate. doi:10.1175/JCLI-D-19-0289.1, 2019.

Colucci, S. J.: Explosive Cyclogenesis and Large-Scale Circulation Changes: Implications for Atmospheric Blocking. J. Atmos. Sci., 42, 2701-2717, doi:10.1175/1520-0469(1985)042<2701:ECALSC>2.0.CO;2, 1985.

Cook, K., Held, I. M.: The Stationary Response to Large-Scale Orography in a General Circulation Model and a Linear Model. J. Atmos. Sci., 49, 525-539, doi:10.1175/1520-0469(1992)049<0525:TSRTLS>2.0.CO;2, 1992.

D'Andrea, F., Tibaldi, S., Blackburn, M., Boer, G., Déqué, M., Dix, M. R., Dugas, B., Ferranti, L., Iwasaki, T., Kitoh, A., Pope, V., Randall, D., Roeckner, E., Strauss, D., Stern, H., Van den Dool, W., and Williamson, D.: Northern Hemisphere atmospheric blocking as simulated by 15 atmospheric general circulation models in the period 1979–1988. Clim. Dynam., 14, 385-407, doi:10.1007/s003820050230, 1998.

Danielson, R. E., Gyakum, J. R., Straub D. N.: A Case Study of Downstream Baroclinic Development over the North Pacific Ocean. Part II: Diagnoses of Eddy Energy and Wave Activity. Mon, Weather Rev., 134, 1549-1567, doi:10.1175/MWR3173.1, 2006

Davini, P., Cagnazzo, C., Gualdi, S., and Navarra, A.: Bidimensional Diagnostics, Variability, and Trends of Northern Hemisphere Blocking. J. Climate, 25, 6496-6509, doi:10.1175/JCLI-D-12-00032.1, 2012.

Dee, D. P., Uppala, S. M., Simmons, A. J., Berrisford, P., Poli, P., Kobayashi, S., Andrae, U., Balmaseda, M. A., Balsamo, G., Bauer, P., Bechtold, P., Beljaars, A. C. M., Van de Berg, L., Bidlot, J., Bormann, N., Delsol, C., Dragani, R., Fuentes, M., Geer, A. J., Haimberger, L., Healy, S. B., Hersbach, H., Hólm, E. V., Isaksen, L., Kållberg, P., Köhler, M., Matricardi, M., McNally, A. P., Monge‐Sanz, B. M., Morcrette, J., Park, B., Peubey, C., de Rosnay, P., Tavolato, C., Thépaut, J., and Vitart, F.: The ERA‐Interim reanalysis: configuration and performance of the data assimilation system. Q. J. Roy. Meteorol. Soc., 137, 553-597, doi:10.1002/qj.828, 2011.

Dole, R., Hoerling, M., Perlwitz, J., Eischeid, J., Pegion, P., Zhang, T., Quan, X., Xu, T., and Murray, D.: Was there a basis for anticipating the 2010 Russian heat wave? Geophys. Res. Lett., 38, n/a, doi:10.1029/2010GL046582, 2011.

Dong, L., Mitra, C., Greer, S., and Burt, E.: The Dynamical Linkage of Atmospheric Blocking to Drought, Heatwave and Urban Heat Island in Southeastern US: A Multi-Scale Case Study. Atmosphere, 9, 33, doi:10.3390/atmos9010033, 2018.

Dunn‐Sigouin, E., Son, S.: Northern Hemisphere blocking frequency and duration in the CMIP5 models. J. Geophys. Res.-Atmos. 118, 1179-1188, doi:10.1002/jgrd.50143, 2013.

E. K. M. Chang, Lee, S., and Swanson, K.L.: Storm Track Dynamics. J. Climate, 15, 2163-2183, doi:10.1175/1520-0442(2002)015<02163:STD>2.0.CO;2, 2002.

Egger, J.: Dynamics of Blocking Highs. J. Atmos. Sci., 35, 1788-1801, doi:10.1175/1520-0469(1978)035<1788:DOBH>2.0.CO;2, 1978.

~~31~~

Frierson, D. M. W.: The Dynamics of Idealized Convection Schemes and Their Effect on the Zonally Averaged Tropical Circulation. J. Atmos. Sci., 64, 1959-1976, doi:10.1175/JAS3935.1, 2007.

Frierson, D. M. W., Held, I. M., and Zurita-Gotor, P.: A Gray-Radiation Aquaplanet Moist GCM. Part I: Static Stability and Eddy Scale. J. Atmos. Sci., 63, 2548-2566, doi:10.1175/JAS3753.1, 2006.

Frierson, D. M. W., Held, I. M., and Zurita-Gotor, P.: A Gray-Radiation Aquaplanet Moist GCM. Part II: Energy Transports in Altered Climates. J. Atmos. Sci., 64, 1680-1693, doi:10.1175/JAS3913.1, 2007.

Geen, R., Lambert, F. H. and Vallis, G. K.: Regime Change Behavior during Asian Monsoon Onset. J. Climate, 31, 3327-3348, doi:10.1175/JCLI-D-17-0118.1, 2018.

Grose, W. L., Hoskins, B. J.: On the Influence of Orography on Large-Scale Atmospheric Flow. J. Atmos. Sci., 36, 223-234, doi:10.1175/1520-0469(1979)036<0223:OTIOOO>2.0.CO;2, 1979.

Guo, Y., Chang, E. K. M., and Leroy, S. S.: How strong are the Southern Hemisphere storm tracks? Geophys. Res. Lett., 36, L22806, doi:10.1029/2009GL040733. 2009.

Hassanzadeh, P., Kuang, Z., and Farrell, B. F.: Responses of midlatitude blocks and wave amplitude to changes in the meridional temperature gradient in an idealized dry GCM. Geophys. Res. Lett., 41, 5223-5232, doi:10.1002/2014GL060764, 2014.

Held, I. M., Ting, M., and Wang, H.: Northern Winter Stationary Waves. J. Climate, 15, 2125-2144, doi:10.1175/1520-0442(2002)015<2125:NWSWTA>2.0.CO;2, 2002.

Hu, Y., Yang, D., and Yang, J.: Blocking systems over an aqua planet. Geophys. Res. Lett., 35, L19818-n/a, doi:10.1029/2008GL035351, 2008.

Hodges, K. I., Lee, R. W., and Bengtsson, L.: A Comparison of Extratropical Cyclones in Recent Reanalyses ERA-Interim, NASA MERRA, NCEP CFSR, and JRA-25. J. Climate, 24, 4888-4906, doi:10.1175/2011JCLI4097.1, 2011.

Luo, D.: A Barotropic Envelope Rossby Soliton Model for Block–Eddy Interaction. Part I: Effect of Topography. J. Atmos. Sci., 62, 5-21, doi:10.1175/1186.1, 2005.

Lutsko, N. J., Held, I. M.: The Response of an Idealized Atmosphere to Orographic Forcing: Zonal versus Meridional Propagation. J. Atmos. Sci., 73, 3701-3718, doi:10.1175/JAS-D-16-0021.1, 2016.

Croci-Maspoli, M., Schwierz, C., and Davies, H. C.: A Multifaceted Climatology of Atmospheric Blocking and Its Recent Linear Trend. J. Climate, 20, 633-649, doi:10.1175/JCLI4029.1, 2007.

Manabe, S., Terpstra, T. B.: The Effects of Mountains on the General Circulation of the Atmosphere as Identified by Numerical Experiments. J. Atmos. Sci., 31, 3-42, doi:10.1175/1520-0469(1974)031<0003:TEOMOT>2.0.CO;2, 1974.

Masato, G., Hoskins, B. J., and Woollings, T. J.: Wave‐breaking characteristics of midlatitude blocking. Q. J. Roy. Meteorol. Soc., 138, 1285-1296, doi:10.1002/qj.990, 2012.

Matsueda, M., Mizuta, R. and Kusunoki, S.: Future change in wintertime atmospheric blocking simulated using a 20-km-mesh atmospheric global circulation model. J. Geophys. Res.-Atmos., 114, D12114-n/a, doi:10.1029/2009JD011919, 2009.

~~32~~

Mattingly, K. S., McLeod, J. T., Knox, J. A., Shepherd, J. M., and Mote, T. L.: A climatological assessment of Greenland blocking conditions associated with the track of Hurricane Sandy and historical North Atlantic hurricanes. International Journal of Climatology, 35, 746-760, doi:10.1002/joc.4018, 2015.

Nabizadeh, E., Hassanzadeh, P., Yang, D., and Barnes, E. A.: Size of the Atmospheric Blocking Events: Scaling Law and Response to Climate Change. Geophys. Res. Lett., 46, 13488-13499, doi:10.1029/2019GL084863, 2019.

Nakamura, H., Nakamura, M., and Anderson, J. L.: The Role of High- and Low-Frequency Dynamics in Blocking Formation. Mon. Weather Rev., 125, 2074-2093, doi:10.1175/1520-0493(1997)125<2074:TROHAL>2.0.CO;2, 1997.

Nakamura, H., Shimpo, A.: Seasonal Variations in the Southern Hemisphere Storm Tracks and Jet Streams as Revealed in a Reanalysis Dataset. J. Climate, 17, 1828-1844, doi:10.1175/1520-0442(2004)017<1828:SVITSH>2.0.CO;2, 2004.

Nakamura, N., Huang, C. S. Y.: Atmospheric blocking as a traffic jam in the jet stream. Science, 361, 42-47, doi:10.1126/science.aat0721, 2018.

O'Gorman, P. A., Schneider, T.: The Hydrological Cycle over a Wide Range of Climates Simulated with an Idealized GCM. J. Climate, 21, 3815-3832, doi:10.1175/2007JCLI2065.1, 2008.

Parsons, S., Renwick, J. A., and McDonald, A. J.: An Assessment of Future Southern Hemisphere Blocking Using CMIP5 Projections from Four GCMs. J. Climate, 29, 7599-7611, doi:10.1175/JCLI-D-15-0754.1, 2016.

Pelly, J. L., Hoskins, B. J.: A New Perspective on Blocking. J. Atmos. Sci., 60, 743-755, doi:10.1175/1520-0469(2003)060<0743:ANPOB>2.0.CO;2, 2003.

Pfahl, S., Schwierz, C., Croci-Maspoli, M., Grams, C. M., and Wernli, H.: Importance of latent heat release in ascending air streams for atmospheric blocking. Nat. Geosci., 8, 610-614, doi:10.1038/ngeo2487, 2015.

Pfahl, S., Wernli, H.: Quantifying the relevance of atmospheric blocking for co‐located temperature extremes in the Northern Hemisphere on (sub‐)daily time scales. Geophys. Res. Lett., 39, n/a, doi:10.1029/2012GL052261, 2012.

Pithan, F., Shepherd, T. G., Zappa, G., Sandu, I.: Climate model biases in jet streams, blocking and storm tracks resulting from missing orographic drag. Geophys. Res. Lett., 43, 7231-7240, doi:10.1002/2016GL069551, 2016.

Quintanar, A. I., Mechoso, C. R.: Quasi-Stationary Waves in the Southern Hemisphere. Part I: Observational Data. J. Climate, 8, 2659-2672, doi:10.1175/1520-0442(1995)008<2659:QSWITS>2.0.CO;2, 1995.

Renwick, J. A.: Persistent Positive Anomalies in the Southern Hemisphere Circulation. Mon. Weather Rev., 133, 977-988, doi:10.1175/MWR2900.1, 2005.

Rex, D. F.: Blocking Action in the Middle Troposphere and its Effect upon Regional Climate. Tellus, 2, 196-211, doi:10.3402/tellusa.v2i3.8546, 1950.

Sausen, R., König, W., and Sielmann, F.: Analysis of blocking events from observations and ECHAM model simulations. Tellus A, 47, 421-438, doi:10.3402/tellusa.v47i4.11526, 1995.

Shutts, G. J.: The propagation of eddies in diffluent jetstreams: Eddy vorticity forcing of 'blocking' flow fields. Q. J. Roy. Meteorol. Soc., 109, 737-761, doi:10.1002/qj.49710946204, 1983

~~33~~

Sillmann, J., Croci-Maspoli, M., Kallache, M., and Katz, R. W.: Extreme Cold Winter Temperatures in Europe under the Influence of North Atlantic Atmospheric Blocking. J. Climate, 24, 5899-5913, doi:10.1175/2011JCLI4075.1, 2011.

Strong, C., Magnusdottir, G.: Tropospheric Rossby Wave Breaking and the NAO/NAM. J. Atmos. Sci., 65, 2861-2876, doi:10.1175/2008JAS2632.1, 2008.

Takaya, K., Nakamura, H.: A Formulation of a Phase-Independent Wave-Activity Flux for Stationary and Migratory Quasigeostrophic Eddies on a Zonally Varying Basic Flow. J. Atmos. Sci., 58, 608-627, doi:10.1175/1520-0469(2001)058<0608:AFOAPI>2.0.CO;2, 2001.

Trenberth, K. E.: Storm Tracks in the Southern Hemisphere. J. Atmos. Sci., 48, 2159-2178, doi:10.1175/1520-0469(1991)048<2159:STITSH>2.0.CO;2, 1991.

Troen, I. B., Mahrt, L.: A simple model of the atmospheric boundary layer; sensitivity to surface evaporation. Bound.-Lay. Meteorol., 37, 129-148, doi:10.1007/BF00122760, 1986.

Tung, K. K., Lindzen, R. S.: A Theory of Stationary Long Waves. Part I: A Simple Theory of Blocking. Mon. Weather Rev., 107, 714-734, doi:10.1175/1520-0493(1979)107<0714:ATOSLW>2.0.CO;2, 1979.

Valdes, P. J., Hoskins, B. J.: Nonlinear Orographically Forced Planetary Waves. J. Atmos. Sci., 48, 2089-2106, doi:10.1175/1520-0469(1991)048<2089:NOFPW>2.0.CO;2, 1991.

Vallis, G. K., Colyer, G., Geen, R., Gerber, E., Jucker, M., Maher, P., Paterson, A., Pietschnig, M., Penn, J., and Thomson, S. I.: Isca, v1.0: a framework for the global modelling of the atmospheres of Earth and other planets at varying levels of complexity. Geosci. Model Dev., 11, 843-859, doi:10.5194/gmd-11-843-2018, 2018.

Wallace, J. M., Lim, G., and Blackmon, M. L.: Relationship between Cyclone Tracks, Anticyclone Tracks and Baroclinic Waveguides. J. Atmos. Sci., 45, 439-462, doi:10.1175/1520-0469(1988)045<0439:RBCTAT>2.0.CO;2, 1988.

Wang, L., Z. Kuang, Z.: Evidence against a general positive eddy feedback in atmospheric blocking. arXiv preprint arXiv:1907.00999. 2019

White, R. H., Battisti, D. S., and Roe, G. H.: Mongolian Mountains Matter Most: Impacts of the Latitude and Height of Asian Orography on Pacific Wintertime Atmospheric Circulation. J. Climate, 30, 4065-4082, doi:10.1175/JCLI-D-16-0401.1, 2017.

Wirth, V., Riemer, M., Chang, E. K. M., and Martius, O.: Rossby Wave Packets on the Midlatitude Waveguide—A Review. Mon. Weather Rev., 146, 1965-2001, doi:10.1175/MWR-D-16-0483.1, 2018.

Woollings, T., Barriopedro, D., Methven, J., Son, S., Martius, O., Harvey, B., Sillmann, J., Lupo, A., Seneviratne, S.: Blocking and its Response to Climate Change. Curr Clim Change Rep, 4, 287-300, doi:10.1007/s40641-018-0108-z, 2018.

Yamazaki, A., Itoh, H.: Vortex–Vortex Interactions for the Maintenance of Blocking. Part I: The Selective Absorption Mechanism and a Case Study. J. Atmos. Sci., 70, 725-742, doi:10.1175/JAS-D-11-0295.1, 2013.

~~34~~

Configuration~~–Region~~	**Region**	**Western Edge**	**Eastern Edge**
Single Mountain (SingleMtn)~~ - East~~	**East**~~10° W~~	**0°**	**90° E**
~~SingleMtn - Mid~~	~~160° W~~	~~60° W~~	
~~SymMtn - East~~	**Other**~~10° W~~	**90° E**	**0°**
Two Mountains (TwoMtn)	~~AsymMtn –~~ **Wide Basin East**	**0°**~~10° W~~	**90° E**
	~~AsymMtn –~~ **Wide Basin Other**~~Mid~~	**150°**~~110°~~ **W**	**0°**~~10° W~~
	~~AsymMtn –~~ **Short Basin**	**90°**~~110°~~ **E**	**150° W**

Table 1: Regions used for subsetting blocks in the compositing and duration~~certain~~ analysis.~~, per model configuration.~~ Each region spans 30°- 65° N, for the longitudes~~100° of longitude~~ listed in the table.

~~35~~

Configuration	~~Area Averaged Block Frequency (%), 30° N- 65° N~~	~~Area Averaged Block Frequency (%), 65° N- 90° N~~	Area Averaged Block Frequency (%), 30° N- 90° N	Number of Events
Aquaplanet	3.24~~1.98~~	387~~1.69~~	~~1.93~~	
1 km single mountain	3.17	365		
~~SingleMtn~~	2 km single mountain ~~2.53~~	3.67~~1.46~~	400~~2.34~~	
3 km single mountain	3.74	438		
4 km single mountain	3.84	433		
Two 3 km mountains (TwoMtn)~~Sym Mtn~~	4~~3~~.01	423~~1.35~~	~~2.71~~	
~~AsymMtn~~	~~2.58~~	~~1.35~~	~~2.36~~	

Table 2: Cool season area~~Area~~-averaged~~, wintertime~~ block ~~occurrence~~ frequency ~~for midlatitudes~~ and number of events~~high-latitudes~~ in the~~all~~ idealized model integrations~~configurations~~.

~~Configuration~~ ~~Number of Events~~	**Mean block duration~~Block Duration~~ (days) and number of events**			~~Mean Block Displacement per 6 hours (km)~~
	All Midlatitude Blocks	**East blocks**		**Other blocks**
Aquaplanet	**7.53 (227)**~~95~~	-~~7.3~~		-~~155.3~~
1 km mountain ~~SingleMtn~~	**7.78 (206)**~~105~~	**8.65 (58)**~~4~~		**7.44 (148)**~~152.6~~
2 km mountain	**7.93 (234)**	**8.54 (75)**		**7.64 (159)**
3 km mountain	**7.55 (266)**	**7.91 (103)**		**7.31 (163)**
4 km mountain	**7.78 (244)**	**7.99 (81)**		**7.68 (163)**
Two 3 km mountains (TwoMtn)~~SymMtn~~	**8.17 (238)**~~139~~	**Wide Basin**	**8.35 (81)**~~0~~	**8.47 (86)**~~150.3~~
		Short Basin ~~7.6~~	**7.65 (68)**~~158.2~~	

Table 3: Mean~~Total count of blocking events mean~~ block duration~~,~~ and number of events in parentheses~~mean block displacement,~~ for midlatitude, cool season ~~winter~~ blocks in each idealized model configuration.

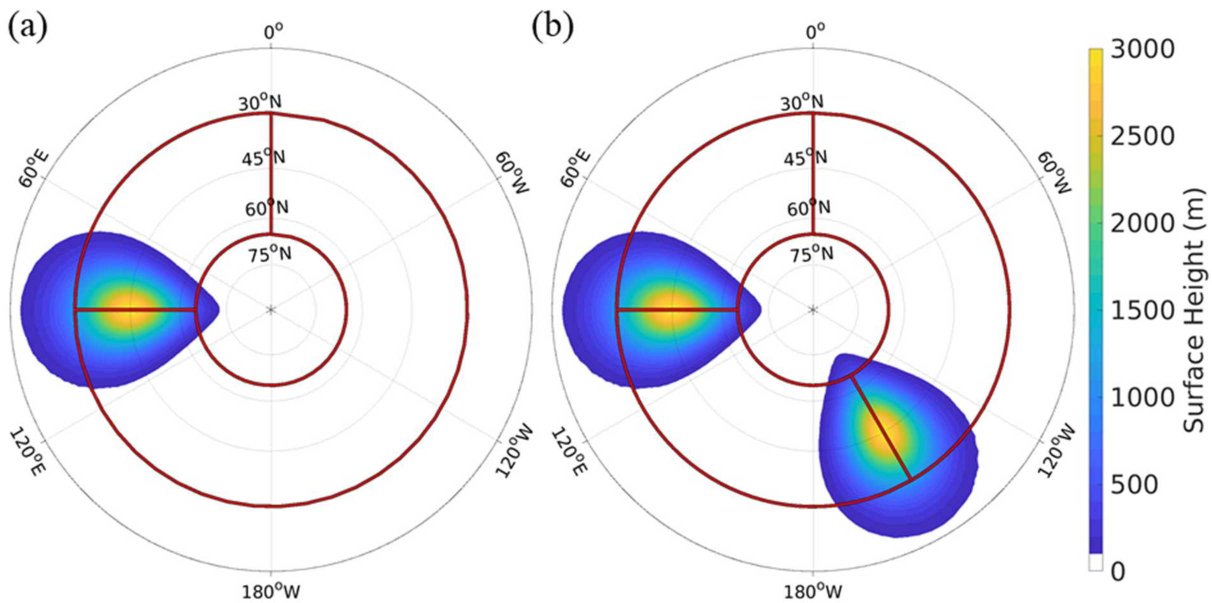

~~Configuration – Region~~	~~Number of Events~~	~~Mean Block Duration (days)~~
~~Aquaplanet – All longitudes~~	~~95~~	~~7.3~~
~~SingleMtn – East~~	~~57~~	~~9.1~~
~~SingleMtn – Mid~~	~~27~~	~~8.2~~
~~SymMtn – East~~	~~51~~	~~8.8~~
~~AsymMtn – Wide Basin East~~	~~42~~	~~8.3~~
~~AsymMtn – Wide Basin Mid~~	~~31~~	~~7.1~~
~~AsymMtn – Short Basin~~	~~50~~	~~7.2~~

~~38~~

~~**Table 4: Average midlatitude winter block duration and number of events for blocks sorted by configuration and select basins as defined in Table 1.**~~

~~39~~

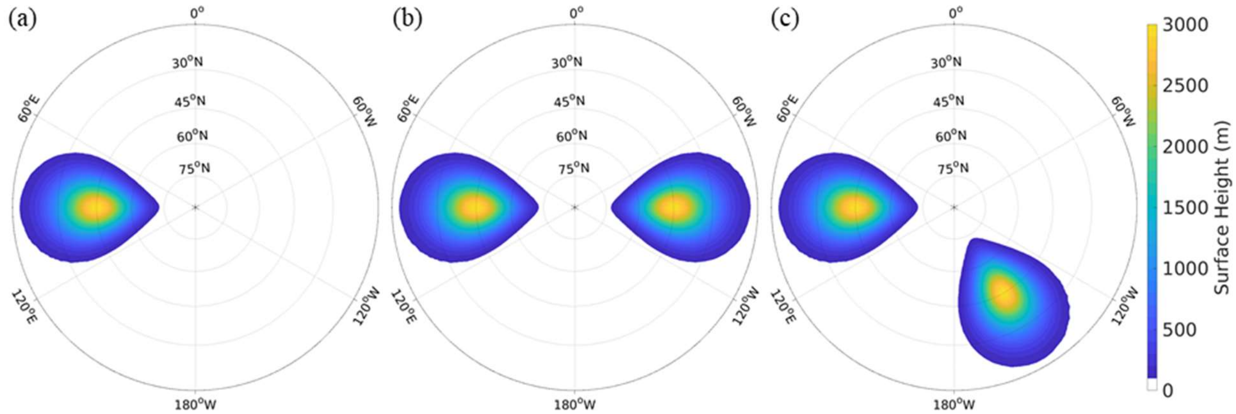

Figure 1: Surface height~~heights~~ (shading) of the ~~3 topographical configurations of the~~ idealized model integrations with~~:~~ (a) a single 3 km high Gaussian mountain centered at 45 N, 90E and~~SingleMtn~~ (b) two 3 km high Gaussian mountains centered at 45 N, 90E and 45 N, 150 W, respectively. The red outlines indicate the block genesis regions described in Table 1.

~~SymMtn (c) AsymMtn.~~

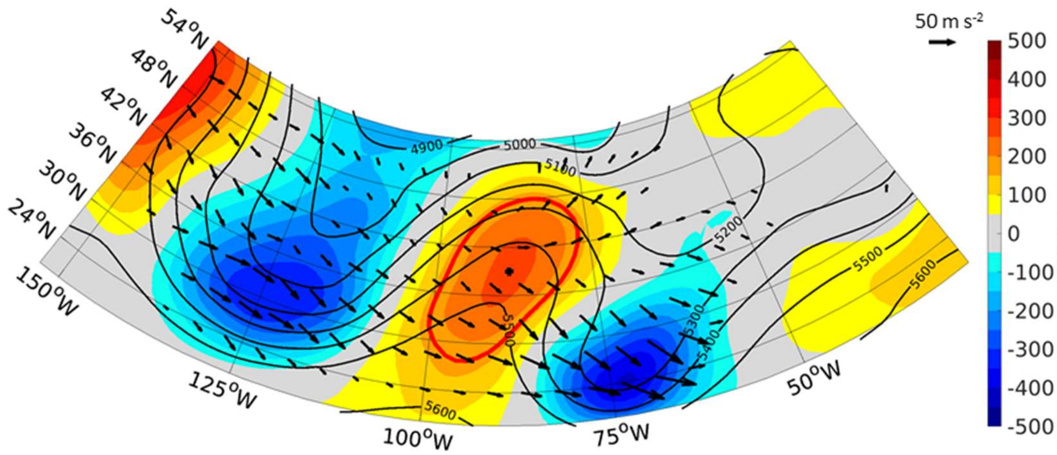

~~41~~

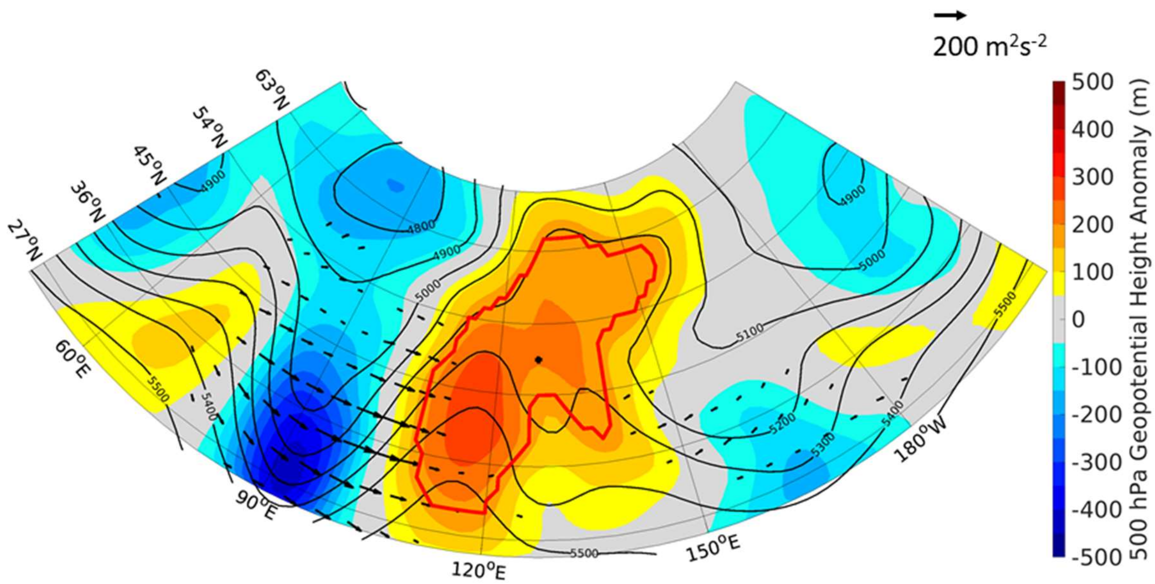

Figure 2: 500 hPa geopotential height (black contours), 500 hPa geopotential height anomaly (shading), outline of blocked area (red contour), and wave activity flux vectors~~,~~ $\vec{W}$ (black arrows), for the first day of a blocking episode in the aquaplanet run. The black dot inside the block denotes the block centroid. Geopotential height contours are in 100 m intervals. ~~Only~~ $\vec{W}$ with magnitudes less~~greater~~ than 20~~25~~ m^2 s^{-2} are removed~~shown~~.

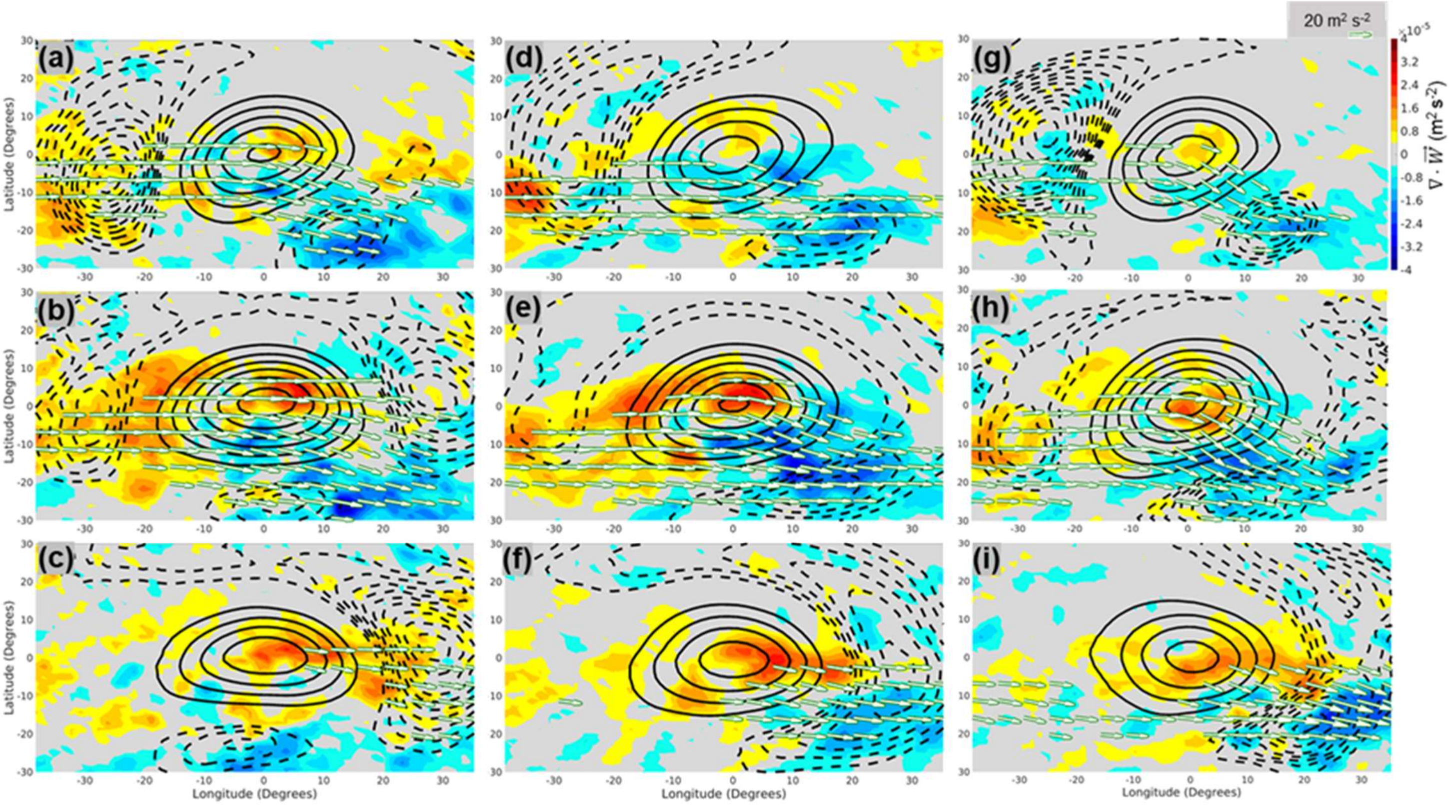

20 m^2 s^{-2}
(a)
(b)
(c)
(d)
(e)
(f)
(g)
(h)
(i)
Latitude (Degrees)
Longitude (Degrees)
$\nabla \cdot \vec{W}$ (m^{2}s^{-2})
$\times 10^{-5}$

~~43~~

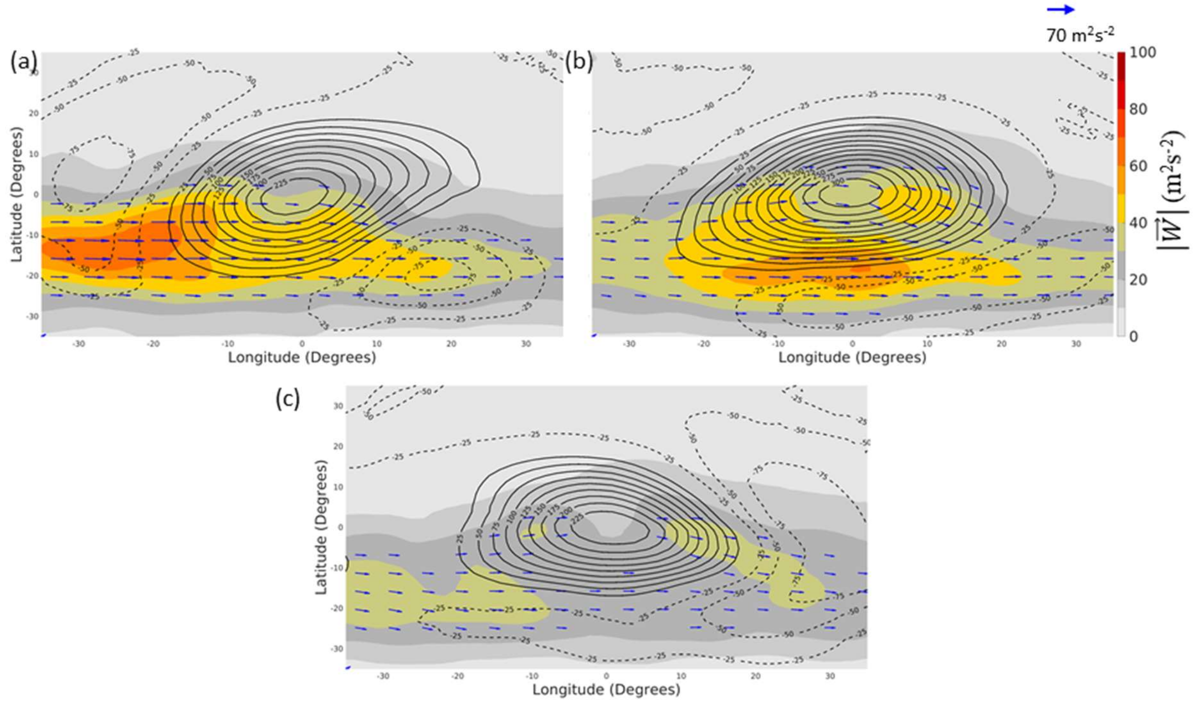

Figure 3: For cool season blocking events: Block centered composites of positive 500 hPa geopotential height anomalies (solid contours), negative 500 hPa geopotential height anomalies (dotted contours), $\vec{W}$ (~~blue~~ arrows), and $\nabla \cdot \vec{W}$ ~~$|\vec{W}|$~~ (shading). (a-c) Left: Computed with SH blocks in ERA-Interim. (d-f) Centre: Computed with) ~~for midlatitude~~ blocks in the aquaplanet integration. (g-i) Right: Computed with blocks in the 3 km single mountain integration. The top, middle, ~~. (a), (b),~~ and bottom rows~~(c)~~ are composites over the first, strongest, and last timesteps of blocking episodes, respectively. Positive (negative) 500 hPa geopotential height anomaly contours are in 50~~25~~ m (-10 m) intervals with outer contour 50 m (-30 m). ~~.~~ $\vec{W}$ with magnitudes less than 20~~25~~ m^2 s^{-2} are removed. Latitude and longitude are defined relative to the composite block center.

44

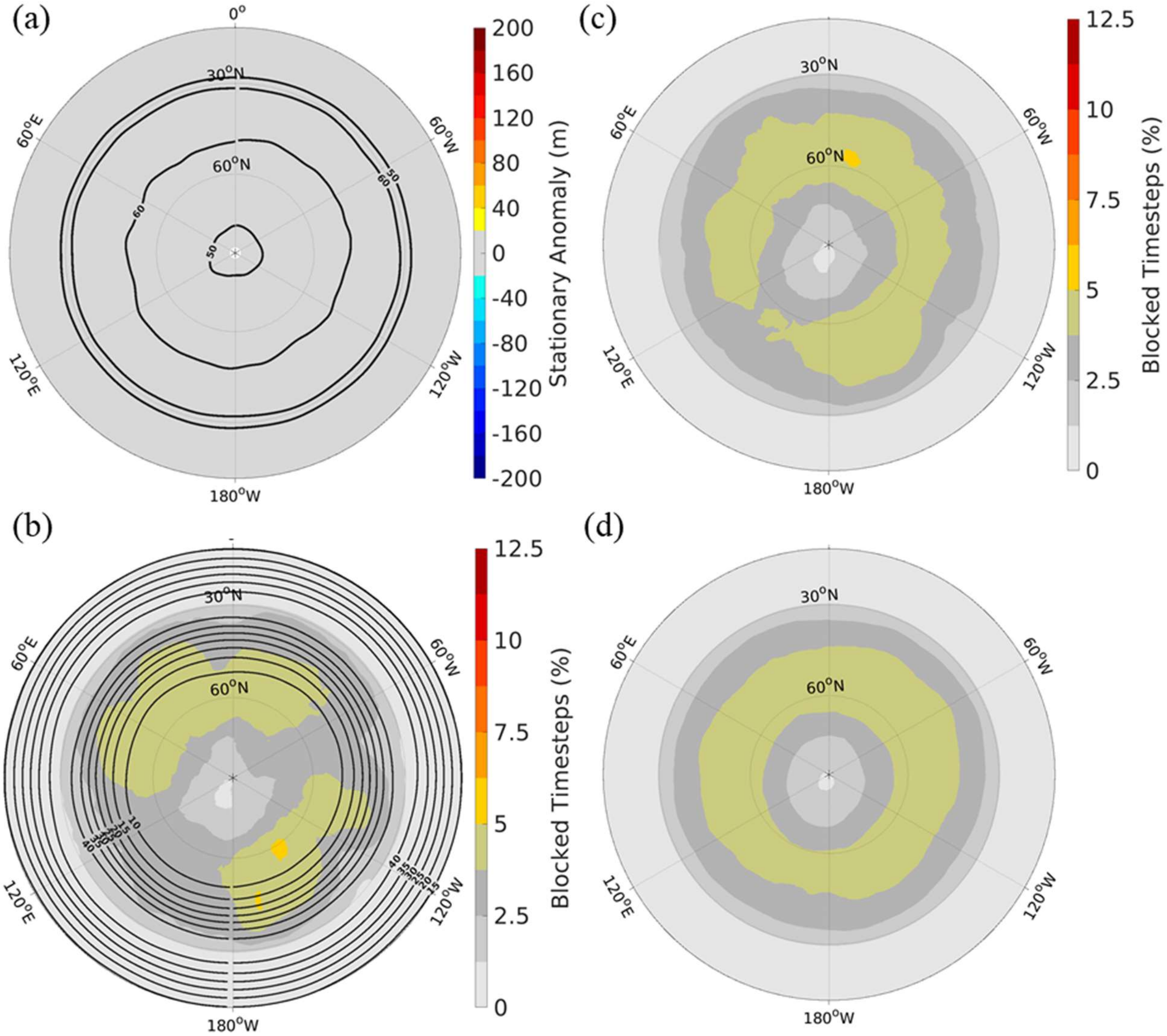
(a)
(b)
(c)
(d)
0°
30°N
60°N
60°E
60°W
120°E
120°W
180°W
Stationary Anomaly (m)
200
160
120
80
40
0
-40
-80
-120
-160
-200
Blocked Timesteps (%)
12.5
10
7.5
5
2.5
0

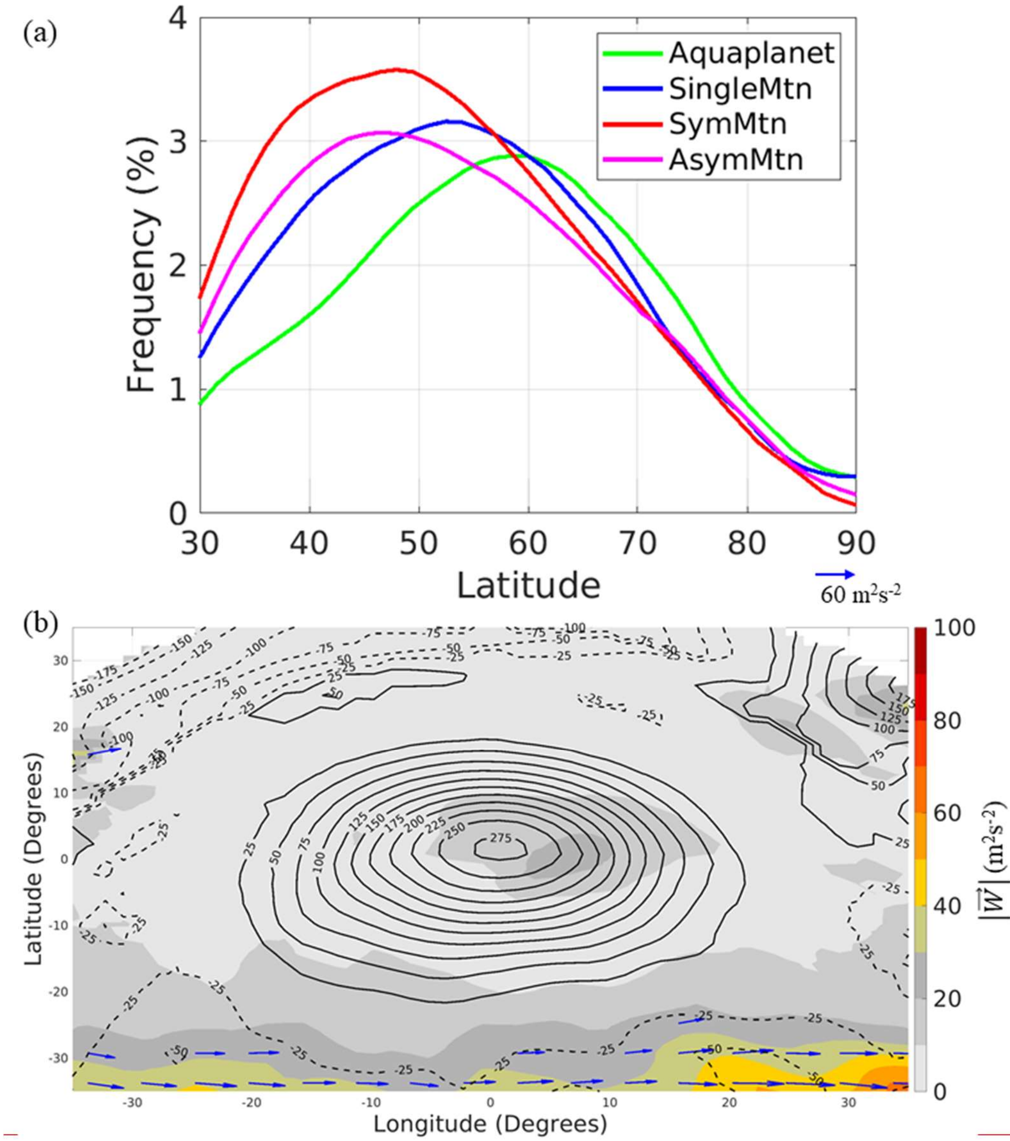

Figure 4: (a and c) Top:) ~~Zonally averaged winter blocking climatology for each model configuration (b)~~ For 30 cool seasons (Nov.-Mar.) in the~~high-latitude~~ aquaplanet ~~blocks during peak intensity, block centered composites of positive 500 hPa geopotential height anomalies (solid contours), negative 500 hPa geopotential height anomalies (dotted contours),~~ ~~$\vec{W}$ (arrows), and $|\vec{W}|$ (shading). 500 hPa geopotential height anomaly contours are in 25 m intervals.~~ ~~$\vec{W}$ with magnitudes less than 25 $m^2 s^{-2}$ are removed.~~

~~46~~

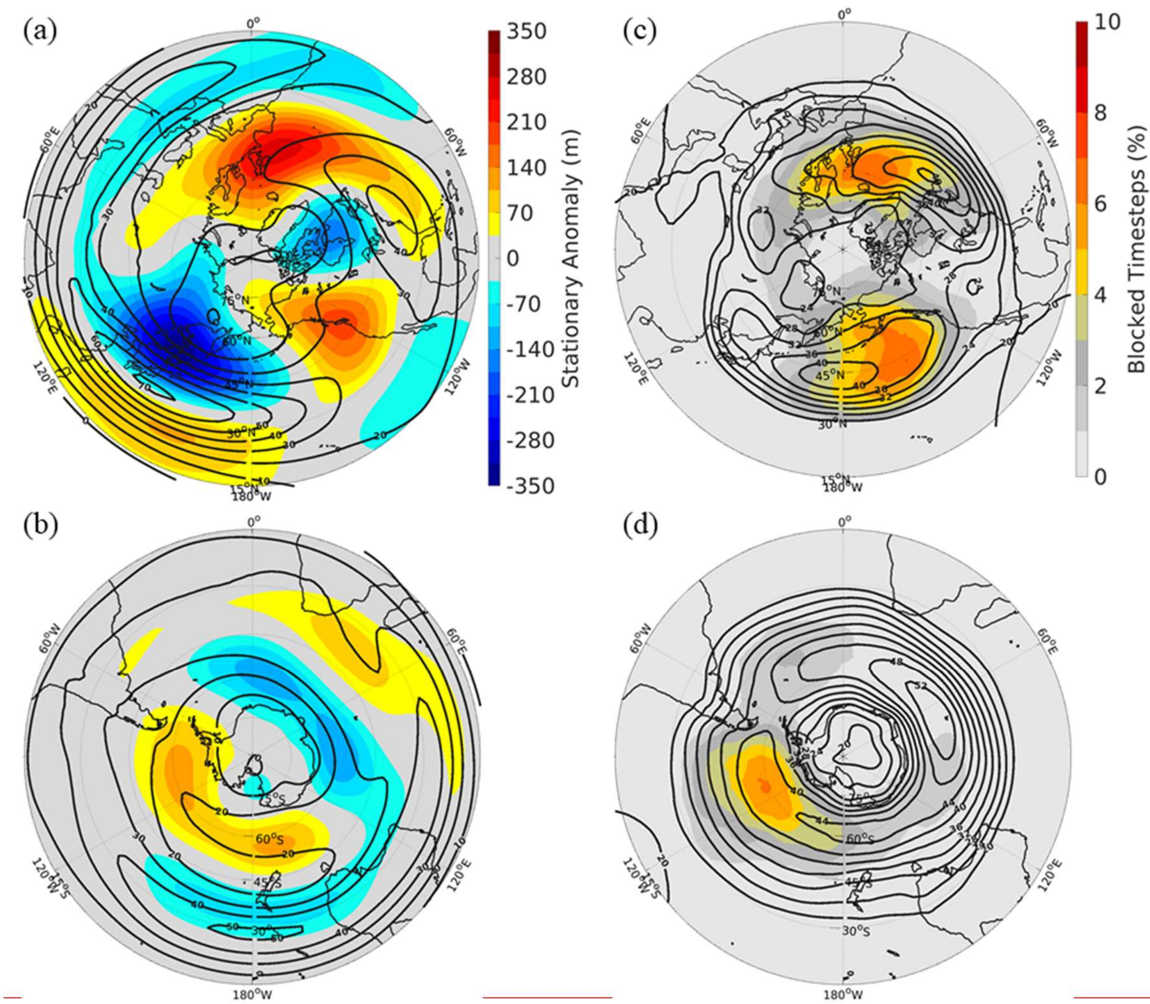

~~Figure 5: (a-b) Left: ~~, (a) the~~Winter~~ stationary wave (shading) and storm track~~U250 climatology~~ (heavy black contours),~~)~~ ~~for the (a) northern~~ and (~~b) southern hemispheres. U250 contours are in 10 m/s intervals. (~~c) the~~-d) Right: Winter~~ blocking climatology (shading) and $\overline{U250}$ (heavy black contours) for the idealized model aquaplanet integration. (b and d) Bottom: ~~storm~~ Blocking climatology (shading) for (c) 100 and (d) 250 cool seasons in the aquaplanet. In (a) storm track contours are in 10 m intervals where the outer contour is 50 m. In (c) $\overline{U250}$ contours are in 5 m/s intervals where the outer contour is 30 m s^{-1}

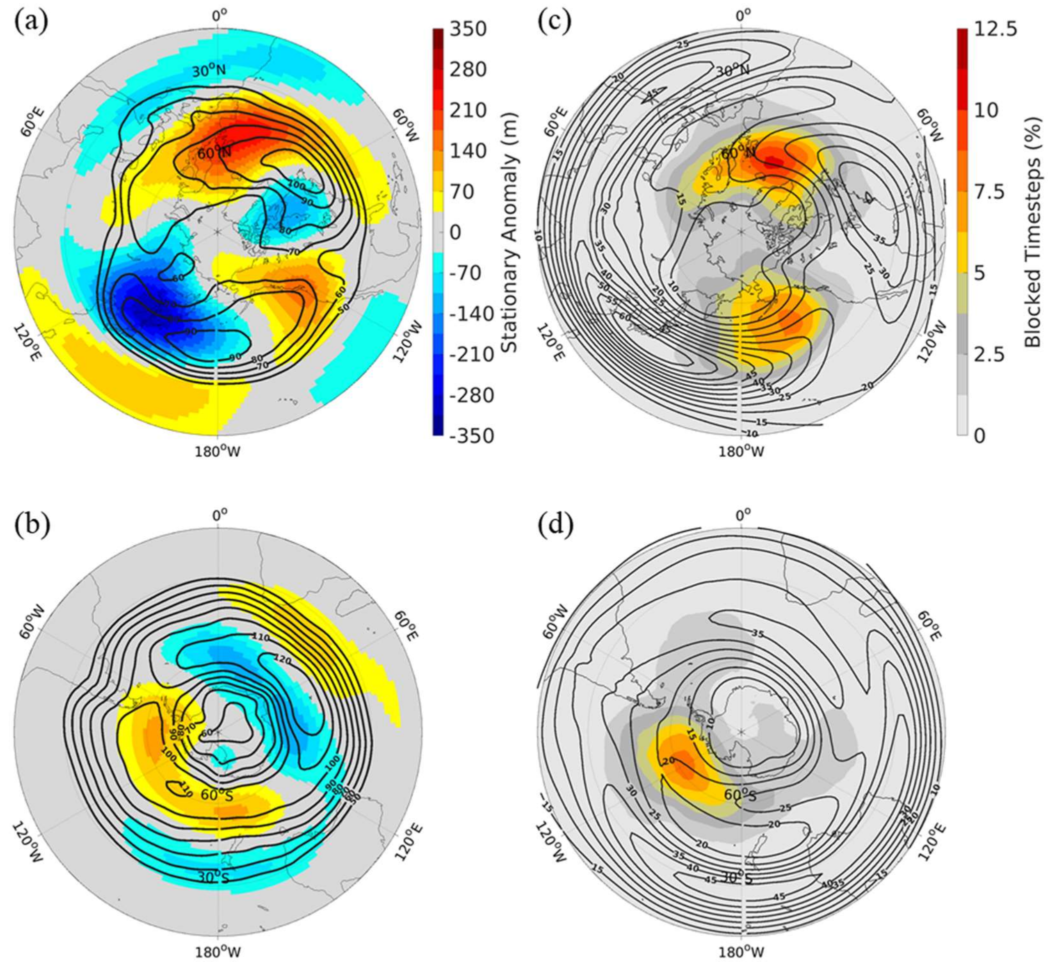

Figure 5: (a-b) Left: Cool season stationary wave (shading) and storm track (heavy black contours) for the (a~~e~~) northern and (b~~d~~) southern hemispheres in ERA-Interim.~~.~~ Storm track contours are in ~~4 m intervals.~~

~~48~~

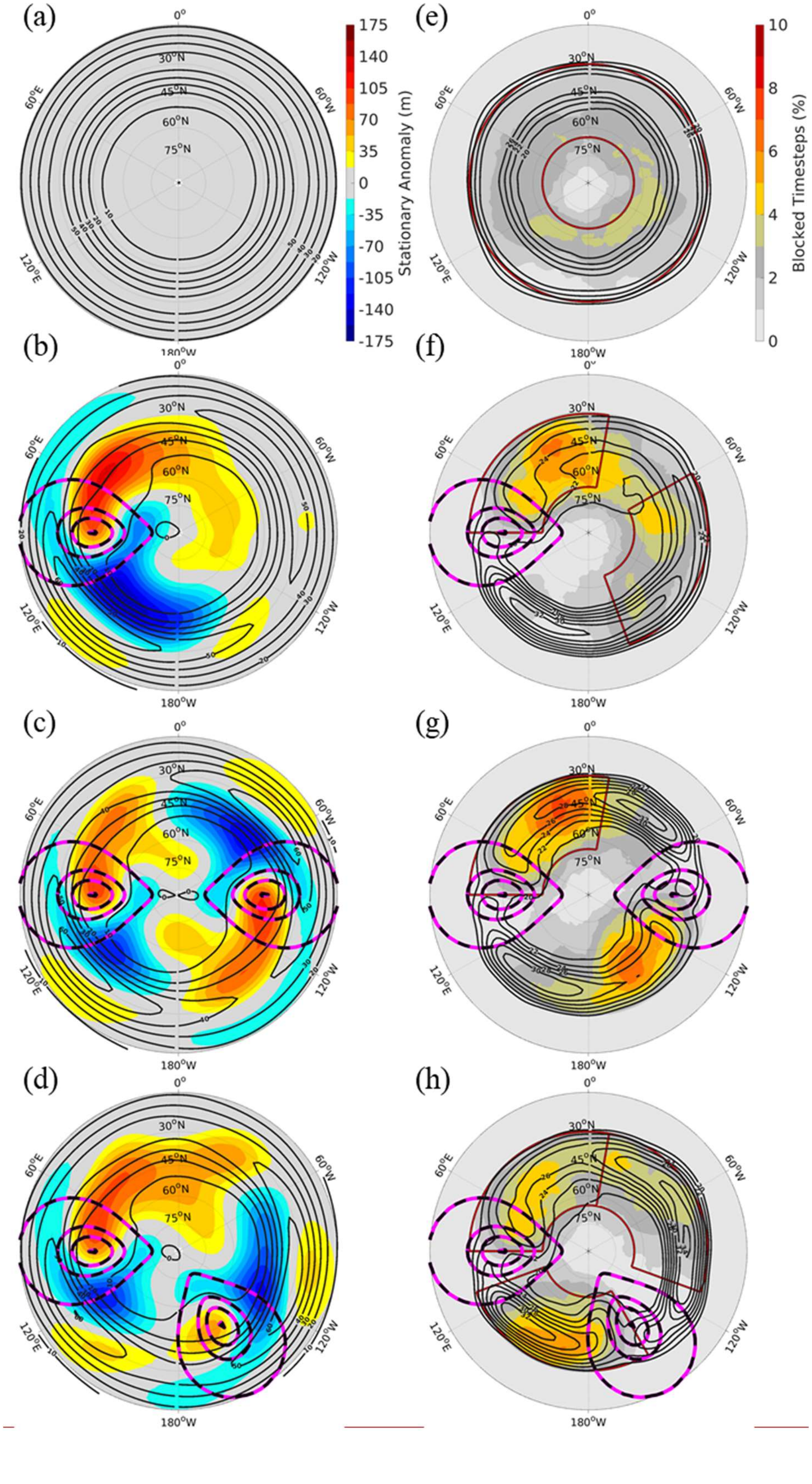

(a)
(b)
(c)
(d)
(e)
(f)
(g)
(h)
Stationary Anomaly (m)
175
140
105
70
35
0
-35
-70
-105
-140
-175
Blocked Timesteps (%)
10
8
6
4
2
0
0°
30°N
45°N
60°N
75°N
60°E
60°W
120°E
120°W
180°W

~~Figure 6: (a-d) Left: Winter stationary wave (shading) and U250 winter climatology (contours) for the (a) aquaplanet (b) SingleMtn (c) SymMtn (d) and AsymMtn. U250 contours are in~~ 10 m~~/s~~ intervals where the outer contour is 50 m. (c-d~~. (e-h~~) Right: Cool season~~Winter~~ blocking climatology (shading) and $\overline{U250}$ (heavy black contours) for the (c) northern and (d) southern hemispheres in ERA-Interim. $\overline{U250}$ contours are in 5 m/s intervals where the outer contour is 10 m s^{-1}.

~~50~~

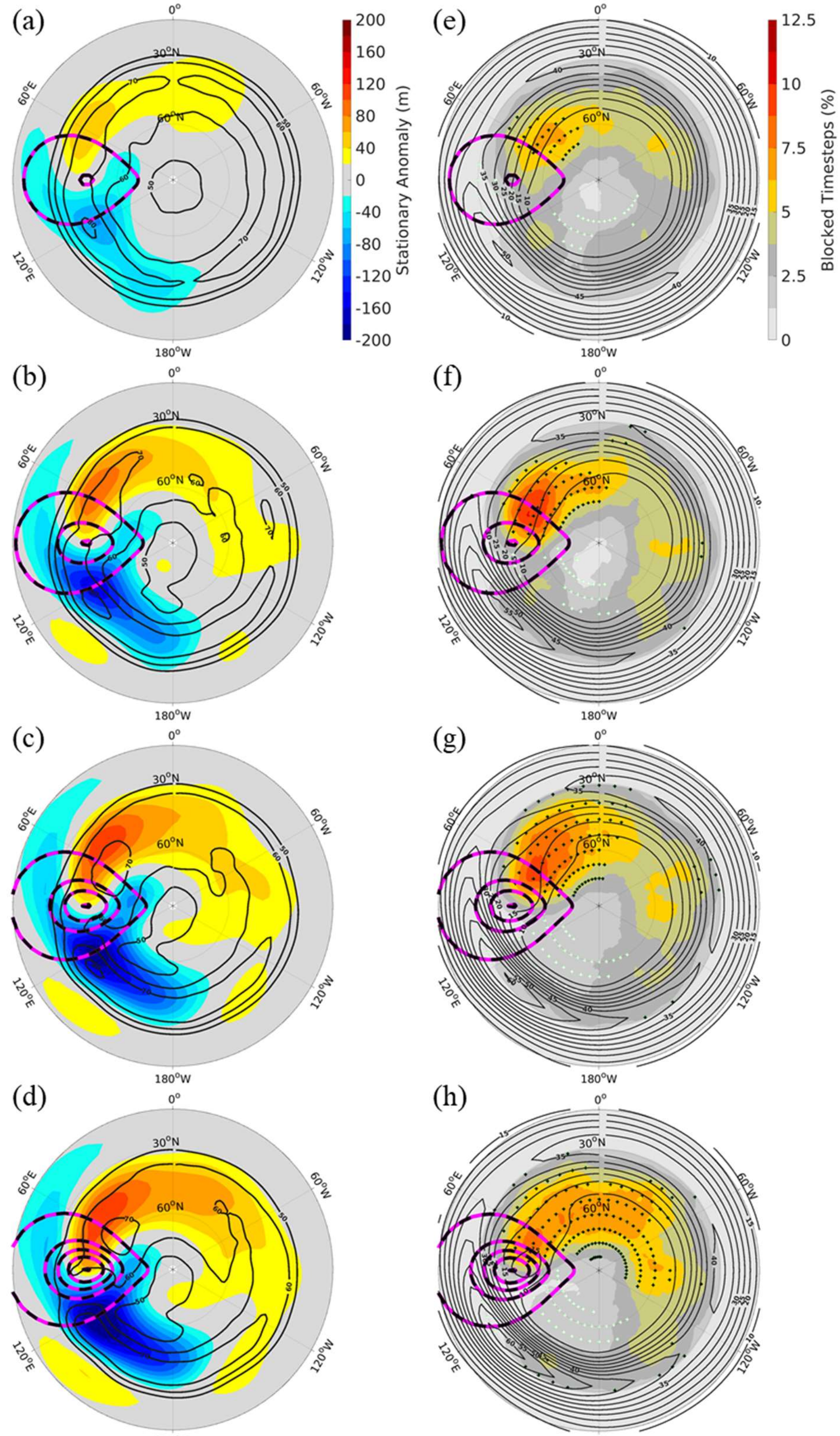
(a)
(b)
(c)
(d)
(e)
(f)
(g)
(h)
0°
30°N
60°N
60°E
60°W
120°E
120°W
180°W
Stationary Anomaly (m)
200
160
120
80
40
0
-40
-80
-120
-160
-200
Blocked Timesteps (%)
12.5
10
7.5
5
2.5
0

Figure 6: (a-d) Left: Cool season stationary wave (shading) and storm track (heavy black contours) for the (a) 1 km, (b) 2 km, (c) 3 km, and (d) 4 km mountain height integrations. Storm track contours are in 10 m intervals where the outer contour is 50 m. (e-h) Right: Cool season blocking climatology (shading) and $\overline{U250}$ (heavy black contours) for the (e) 1 km, (f) 2 km, (g) 3 km, and (h) 4 km mountain height integrations. $\overline{U250}$ contours are in 5 m/s intervals where the outer contour is 10 m s^{-1}. Black (white) stippling in (e-h) indicates significantly greater (less) block frequency at nearby gridpoints when compared to a 250-year aquaplanet integration. Pink and black dotted contours represent surface height, where the outer contour is the edge of the land-mask and the inner contours are in 1 km intervals.

~~52~~

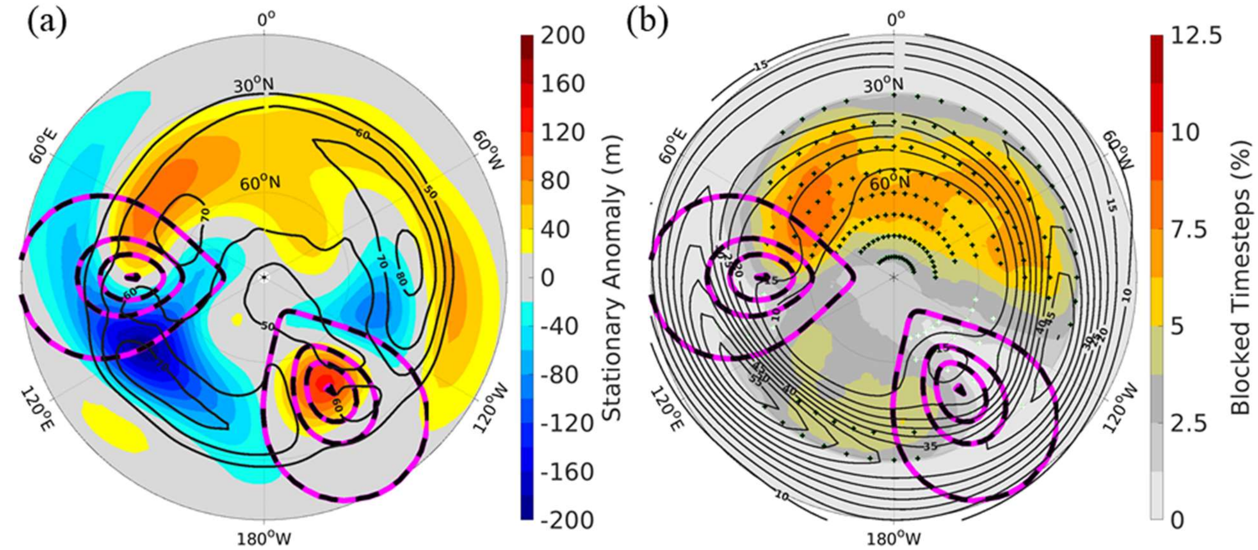

Figure 7: For the 2-mountain idealized model integration, (a) the cool season stationary wave (shading) and storm track (heavy black contours), and (b) the cool season blocking climatology (shading) and $\overline{U250}$ (heavy black contours). In (a) storm track contours are in 10 m intervals where the outer contour is 50 m. In (b) $\overline{U250}$ contours are in 5 m/s intervals where the outer contour is 10 m s^{-1}. Black (white) stippling in b indicates significantly greater (less) block frequency at nearby gridpoints when compared to a 250-year aquaplanet integration.~~storm-track (contours). Storm-track contours are in 2 m intervals.~~ **Pink and black dotted contours represent surface height, where the outer contour is the edge of the land-mask and the inner contours are in 1 km intervals**~~, and the inner contours represent 1, 2, 3 km respectively. Results are presented for (e) aquaplanet (f) SingleMtn (g) SymMtn (h) AsymMtn. The red outlines in the e-h indicate the regions used when separating blocks by region~~.

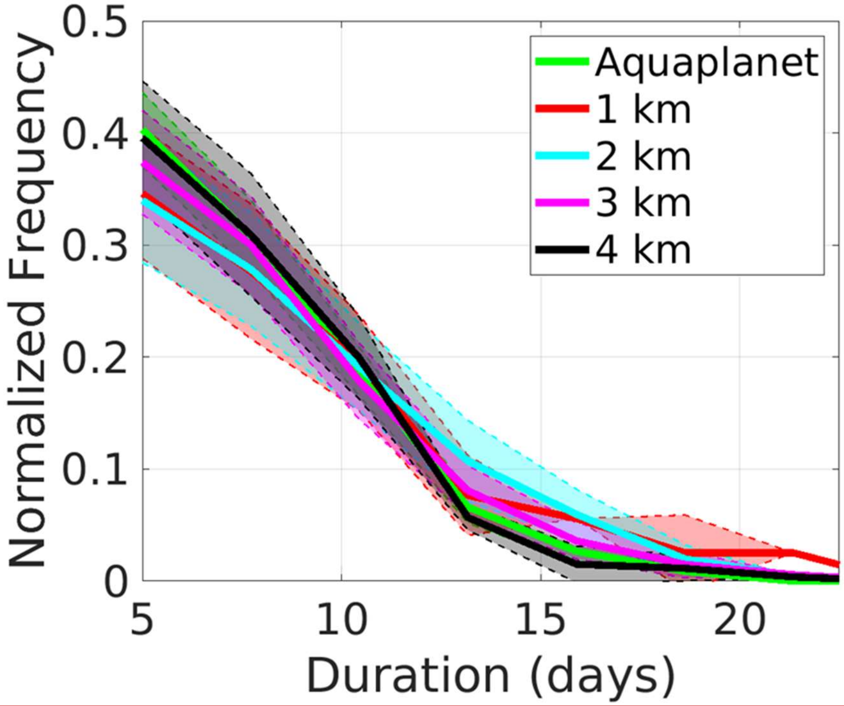
Normalized Frequency
Duration (days)
Aquaplanet
1 km
2 km
3 km
4 km
0
0.1
0.2
0.3
0.4
0.5
5
10
15
20

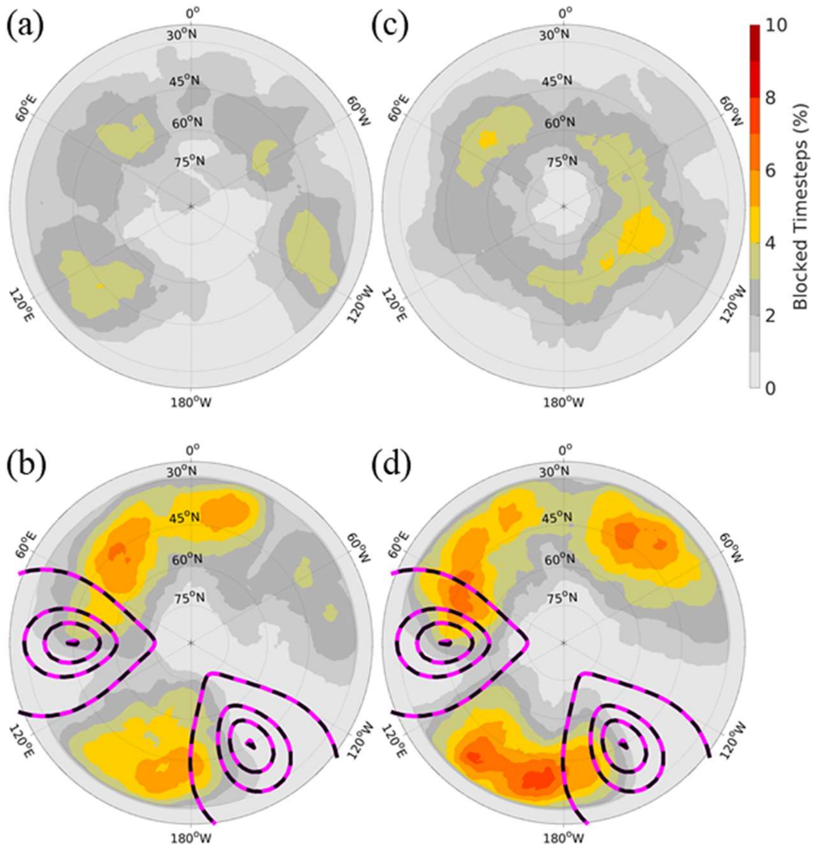

~~Figure 7: Winter blocking climatologies (shading) computed by randomly sampling (a, c) 15 years of years 11-40 in the aquaplanet, and (b, d) 15 years of years 11-40 in AsymMtn. Pink and black dotted contours represent surface height, where the outer contour is the edge of the land-mask, and the inner contours represent 1, 2, 3 km respectively.~~

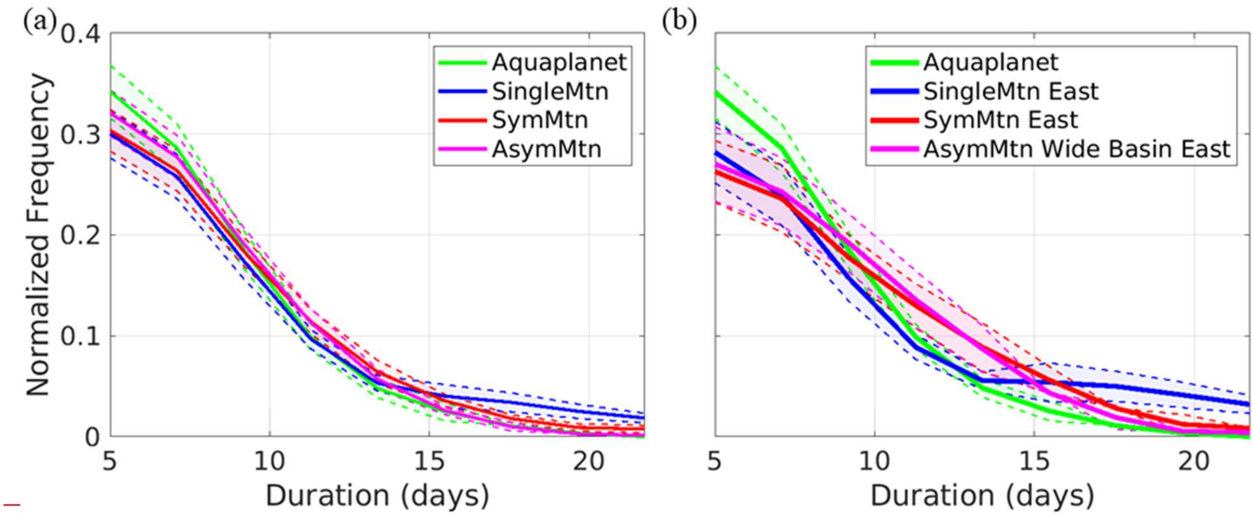

Figure 8: ~~Normalized~~ **Block duration probability density distributions~~Duration Probability Density Distributions~~ for the aquaplanet and "East"~~(a) all winter~~ blocks (as defined in table 1) in the single mountain configurations.~~within each model configuration, and (b) Aquaplanet and just the East blocks for each topographic configuration.~~ Thick ~~colored~~ lines denote the mean probability density distribution for each configuration. Shaded regions bordered by dotted lines outline +/- 1 full~~half a~~ standard deviation from the mean.**

~~56~~

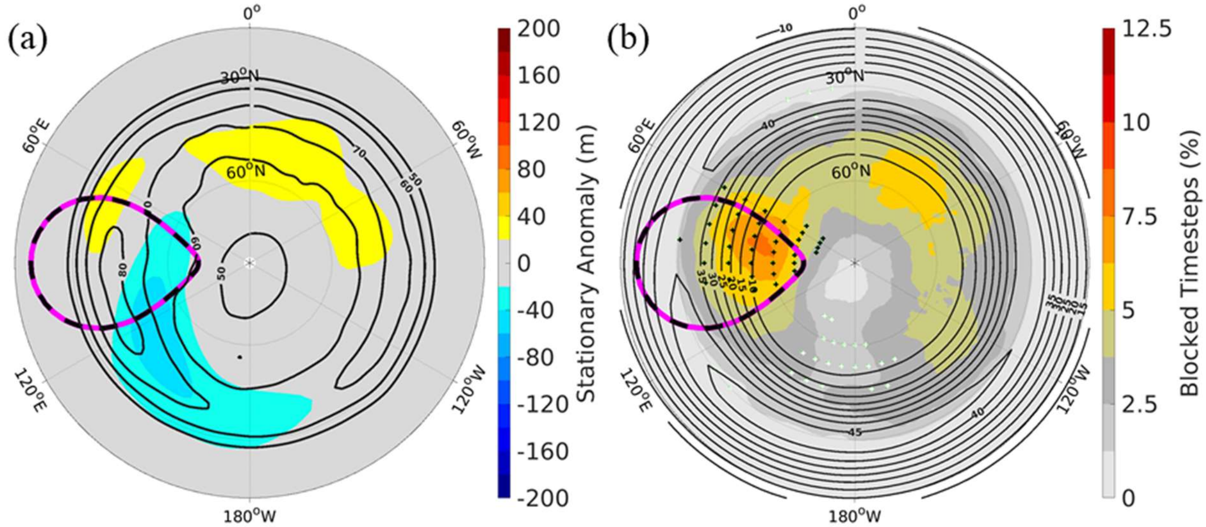

Figure 9: For an integration with 1 flat landmass, (a) the cool season stationary wave (shading) and storm track (heavy black contours), and (b) the cool season blocking climatology (shading) and $\overline{\boldsymbol{U250}}$ (heavy black contours). In (a) storm track contours are in 10 m intervals where the outer contour is 50 m. In (b) $\overline{\boldsymbol{U250}}$ contours are in 5 m/s intervals where the outer contour is 10 m s^{-1}. Black (white) stippling in b indicates significantly greater (less) block frequency at nearby gridpoints when compared to a 250-year aquaplanet integration. The pink and black dotted contours represent the outer edge of the

~~57~~

land-mask.

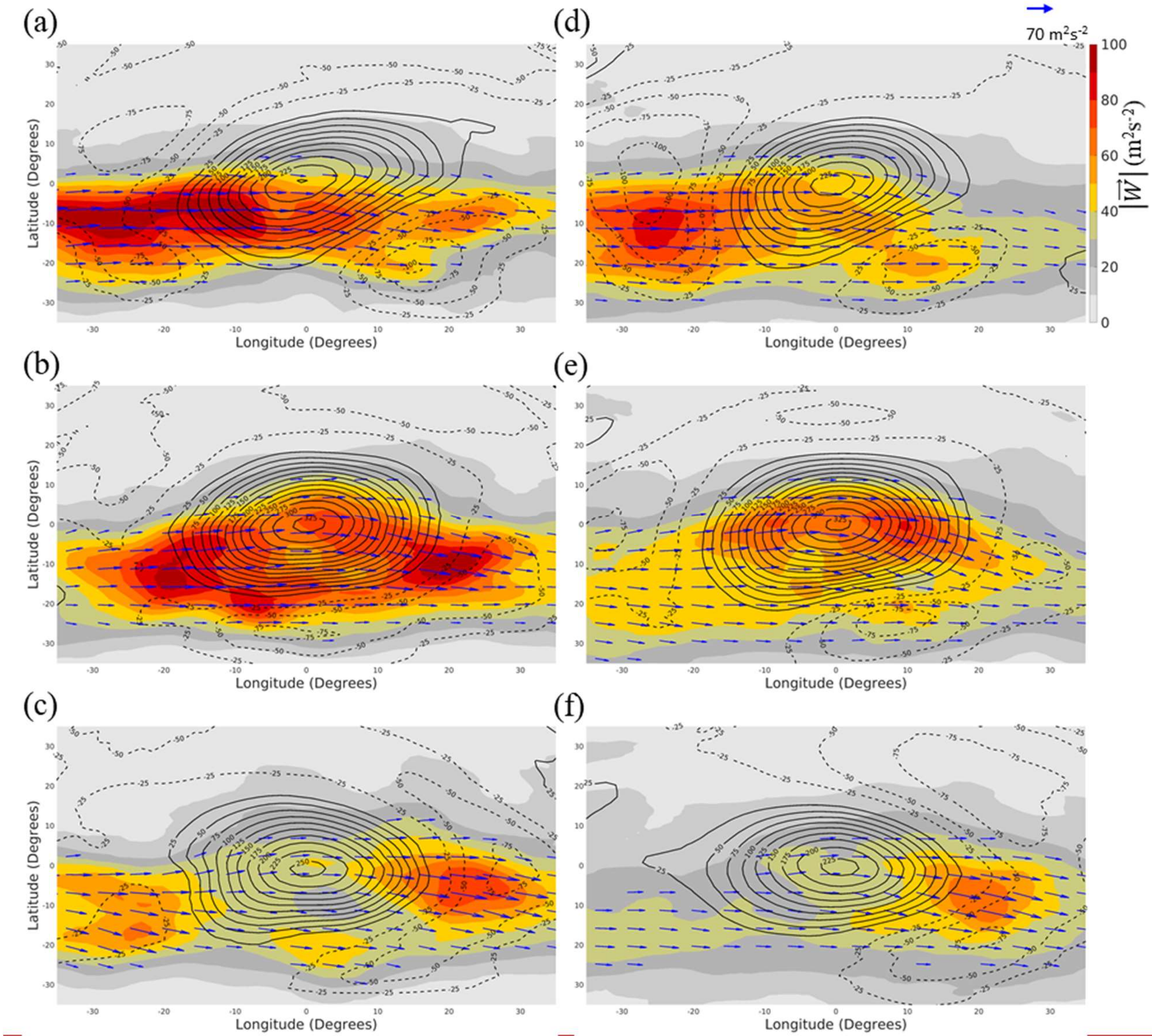

~~**Figure 9: Block centered composites of positive 500 hPa geopotential height anomalies (solid contours), negative 500 hPa geopotential height anomalies (dotted contours), $\vec{W}$ (blue arrows), and $|\vec{W}|$ (shading) for (a-c) Left: SingleMtn midlatitude Mid and (d-f) Right: SingleMtn midlatitude East blocks. The top panel (a, d), middle panel (b, e), and bottom panel (c, f) are composites over the first, strongest, and last timesteps of blocking episodes, respectively. 500 hPa geopotential height anomaly contours are in 25 m intervals. $\vec{W}$ with magnitudes less than 25 m^2 s^{-2} are removed.**~~

~~58~~